

Master's Thesis

Encounter-type Thermal Haptic Device
Using Multiple Rotating Pre-heated Peltier
Actuators

Hoseok Jung (정 호 석)

Department of Computer Science and Engineering

Pohang University of Science and Technology

2023

회전하는 다수의 예열된 펠티어 구동기를
사용한 조우형 열감 햅틱 장치

Encounter-type Thermal Haptic Device
Using Multiple Rotating Pre-heated Peltier
Actuators

Encounter-type Thermal Haptic Device Using Multiple Rotating Pre-heated Peltier Actuators

by

Hoseok Jung

Department of Computer Science and Engineering
Pohang University of Science and Technology

A thesis submitted to the faculty of the Pohang University of
Science and Technology in partial fulfillment of the requirements
for the degree of Master of Science in the Computer Science and
Engineering

Pohang, Korea

07. 31. 2023

Approved by

Seungmoon Choi (Signature)

Academic advisor

Encounter-type Thermal Haptic Device Using Multiple Rotating Pre-heated Peltier Actuators

Hoseok Jung

The undersigned have examined this thesis and hereby certify
that it is worthy of acceptance for a master's degree from
POSTECH

07. 31. 2023

Committee Chair Seungmoon Choi (Seal)

Member Inseok Hwang (Seal)

Member Wooksung Kim (Seal)

MCSE
20212121

정 호 석 Hoseok Jung

Encounter-type Thermal Haptic Device Using Multiple Rotating Pre-heated Peltier Actuators.

회전하는 다수의 예열된 펠티어 구동기를 사용한 조우형 열감 햅틱 장치.

Department of Computer Science and Engineering , 2023,
??p

Advisor : Seungmoon Choi.

Text in English.

ABSTRACT

When users interact with different objects using their hands in a virtual environment, providing thermal haptic feedback offers significant improvements to the overall user experience. However, there are situations that existing thermal haptic devices struggle to accurately represent. One such situation is when touching two or more objects with significantly different initial temperatures. Reducing the latency in reaching the target temperature enhances the user's interaction experience in the virtual environment. To address this, we designed a thermal haptic device to reduce the latency time in initial temperature changes and provide thermal feedback in an encounter-type manner. Our haptic device utilizes multiple Peltier components and a pre-heating system. Our research presents an average faster thermal rendering algorithm compared to conventional using a single thermal display. Through experimentation, we have

demonstrated that this approach enhances the overall user experience when applied in a virtual environment.

Contents

I. Introduction	1
II. Related Work	3
2.1 Thermal Sensory System	3
2.2 Thermal Model for Hand-Object Contact	4
2.3 Thermal Haptic Devices in VR/AR	6
III. Peltier Actuator and Thermal Rendering	8
3.1 Peltier Actuator	8
3.2 Thermal Rendering	13
3.3 Simulation	19
3.3.1 Implementation	19
3.3.2 Comparison with Ho's Model	21
3.3.3 Comparison with Measured Data	24
3.3.4 Utilization of the Simulation	27
IV. Multiple Rotating Pre-heated Peltier Actuators	28
4.1 Hardware Implementation	28
4.2 Software Implementation	31
4.2.1 Lumped System	31
4.2.2 Thermal Analysis of Objects Composed of Composite Materials	32
4.3 Use Scenario	32
4.3.1 Preparing for Collision	32
4.3.2 Controlling Haptic Effects During Contact	35
4.3.3 Grasping and Releasing Object	36

V. User Experiments	37
5.1 Methods	37
5.1.1 Participants	37
5.1.2 Experimental Conditions	37
5.1.3 Evaluation	47
5.1.4 Task and Precedure	47
5.2 Result	48
5.3 Discussion	50
VI. Example Applications	51
6.1 Social Apps	51
6.2 Education	52
6.3 Simulator	53
VII. Conclusion and Future Work	54
7.1 Conclusion	54
7.2 Limitations	54
7.3 Future Work	55
Summary (in Korean)	57

List of Figures

1.1	The Appearance of Haptic Device Developed for Our Research	1
2.1	Layers During Contact between Skin and Object	3
2.2	Example Temperature Graph Over Time During Contact between Skin and Object	4
3.1	Peltier Actuator	8
3.2	Structure of the Peltier Actuator	10
3.3	Temperature Measurement Results During Cooling and Heat Dissipa- tion of the Peltier Actuator	12
3.4	An Overview of Thermal Rendering Using the Peltier Actuator	13
3.5	Temperature rendering results for aluminum with different target tem- peratures	16
3.6	Temperature rendering results for granite with different target temper- atures	16
3.7	Temperature rendering results for glass with different target temperatures	17
3.8	Temperature rendering results for acrylic with different target temper- atures	17
3.9	Temperature rendering results for glass with different target temperatures	19
3.10	Finite element analysis results for aluminum with different temperatures	22
3.11	Finite element analysis results for granite with different temperatures .	22
3.12	Finite element analysis results for glass with different temperatures . .	23
3.13	Finite element analysis results for acrylic with different temperatures .	23
3.14	Simulation results for aluminum with different temperatures	25
3.15	Simulation results for granite with different temperatures	25

3.16	Simulation results for glass with different temperatures	26
3.17	Simulation results for acrylic with different temperatures	26
3.18	Temperature Simulation Results for Aluminum with Varying Temperatures Using a Peltier Actuator with a Cooling Rate Twice as Fast	27
4.1	System diagram of multiple rotating pre-heated Peltier actuators	28
4.2	Dimension of the device components	29
4.3	Appearance of the wearable Hardware	30
4.4	Temperature Parameter Setting Screen in Unity Program	31
4.5	Appearance of the Multiple Rotating Pre-heated Peltier Actuators Depending on the Position of the Virtual Hand and Object in the Virtual Environment	33
4.6	Temperature range and reference temperature of each Peltier in the multiple rotating pre-heated Peltier actuators	33
4.7	Appearance When the Closest Material Changes	34
4.8	Appearance When the Virtual Hand Touches the Virtual Object	35
4.9	Example of Grasp and Ungrasp Operation Depending on the Contact of the Touch Sensor	36
5.1	Comparison of Latency Time Based on Temperature for Two Algorithms	38
5.2	Scenario 1 : Granite Stones	39
5.3	Scene1 thermal stimulis	39
5.4	Thermal rendering results of granite stones	40
5.5	Scenario 2 : Dining Table	41
5.6	Scene2 Stimuli	42
5.7	Thermal rendering results of kimchi soup, mug cup and steak	43
5.8	Thermal rendering results of wine glass, beer can and coke can	44
5.9	Thermal rendering results of water bottle, wine bottle, spoon and chopsticks	45
5.10	Thermal rendering results of riceball and dumpling	46

5.11	User experiment result(* mean $p < 0.05$, ** mean $p < 0.01$)	49
6.1	We designed a game that allows users to engage in snow fighting, and experience social skinship	51
6.2	In this demonstration, we simulated a scenario where a fire occurs indoors	52
6.3	Our space simulation which enables users to interact with objects synchronized with the gravitational forces and atmospheric temperatures of external planets	53
7.1	Thermal Rendering Results at 10 Degrees of Aluminum with Reduced Contact Area	56

I. Introduction

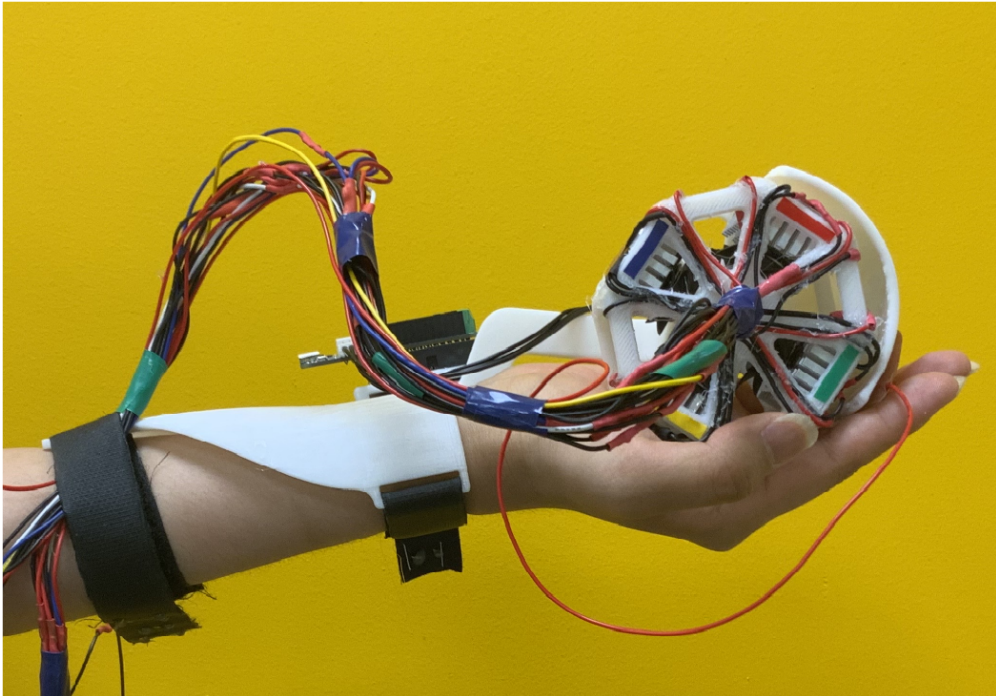


Figure 1.1: The Appearance of Haptic Device Developed for Our Research

Using haptic thermal devices to provide users experiencing virtual environments with realistic thermal feedback as anticipated enhances their immersion [?, ?]. Various research has been conducted to provide appropriate feedback when picking up virtual objects. Devices have been introduced to simulate a range of experiences, such as force, texture, shape, and texture [?, ?, ?, ?, ?, ?]. Research regarding thermal haptic devices to represent heat exchange in virtual environments have also been carried [?, ?, ?, ?, ?]. One of the challenging issues in providing realistic temperature feed-

back during interactions between objects and the hand in virtual spaces is to appropriately offer the experience of touching materials with vastly different temperatures with skin [?]. To provide a realistic heat exchange experience, the thermal display providing thermal feedback should be set differently depending on the initial temperature of the touching scenario. Each of these thermal displays has a limit to temperature changes. As a result, the greater the initial temperature difference, the longer the delay for the thermal display to execute the command. The aim of this research is to propose wearable devices and algorithms that can reduce this delay time compared to existing methods. A haptic device was developed by attaching four peltier components to a cylindrical support and rotating the support to quickly change the peltier component that comes into contact with the user's palm.; see Figure 1.1.

Compared to using a single thermal display, this approach maintains different initial temperatures for each component, allowing for faster temperature increase or decrease in the user's palm to reach the desired initial contact temperature. Additionally, the contact device was designed as an "encountered type" so that it does not provide any stimulation to the palm when not in contact with virtual objects [?]. It quickly moves into contact with the palm to deliver thermal feedback when contact occurs.

The academic contributions of this paper are as follows:

- We presented a method achieving the changes in initial temperature conditions faster than then conventional methods.
- Through user testing, we have proven that reducing the latency time enhances the overall user experience in VR environments.
- This research proposes a multimodal system capable of providing thermal feedback and force feedback in an encounter-type simultaneously.

II. Related Work

2.1 Thermal Sensory System

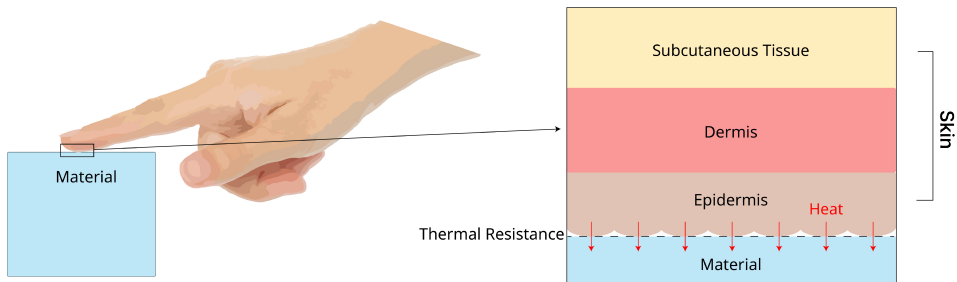


Figure 2.1: Layers During Contact between Skin and Object

The skin is composed of multiple layers, with the outermost layer (epidermis) having a depth of about 1.3 mm at palms and feet [?]. The second layer (dermis) has a thickness of about 1 to 4 mm and includes receptors for touch, pressure, temperature changes, and painful stimuli. Skin sensitivity to temperature varies depending on the body region and the current skin temperature. Humans can perceive temperature due to the presence of two different types of nerve endings in the epidermis [?]. . When the temperature rises, thermoreceptors for warmth are activated, while thermoreceptors for cold are activated when the temperature drops. Both receptors adapt quickly within the range of 30-36 °C. If the rate of skin temperature change is slower than 0.5 °C/minute, temperatures within this range are not perceived as cold or hot [?]. If the skin temperature remains above 36 degrees or below 30 °C, the sensation of heat or cold persists. When the skin temperature exceeds 45 °C or falls below 15 °C, no-

cioreceptors respond to the extreme thermal stimuli. This stimuli causes users to feel pain [?, ?]. Cold afferent fibers are most actively discharged at a skin temperature of $25\text{ }^{\circ}\text{C}$ in cold environments, while warm afferent fibers discharge most actively at $45\text{ }^{\circ}\text{C}$ [?]. Generally, the body is more sensitive to cold stimuli than warm stimuli, and it is more sensitive to changes in skin temperature than absolute temperature itself [?]. Warm and cold fibers are not particularly sensitive to detecting absolute temperatures, but they excel in detecting changes in the temperature of objects. Rapid changes in skin temperature elicit dynamic responses from thermoreceptors. The skin is sensitive to temperature changes, with the most temperature-sensitive part of the hand being the thenar eminence. The thenar eminence can distinguish between two cold temperature stimuli in the range of $0.02\text{-}0.07$ degrees and between two hot temperature stimuli in the range of $0.03\text{-}0.09$ degrees [?, ?, ?]. Skin temperature exhibits interindividual variability, meaning it can vary depending on the individual and the measurement method used [?, ?].

2.2 Thermal Model for Hand-Object Contact

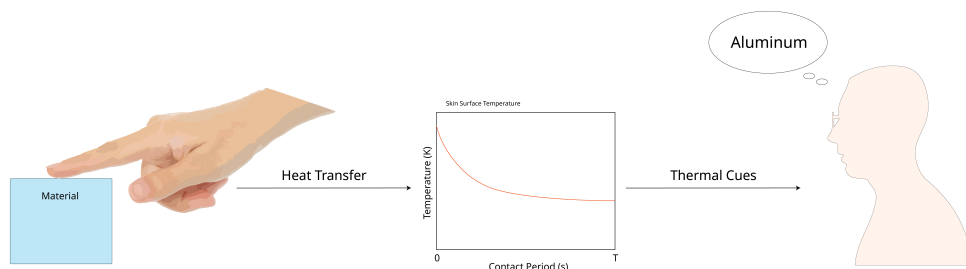


Figure 2.2: Example Temperature Graph Over Time During Contact between Skin and Object

When humans grasp an object, they can infer its material from the temperature

changes sensed on their skin. Regarding the interaction between the hand and an object, most objects show similar patterns. with a sharp temperature change perceived initially when grasped and a gradual decrease in temperature change over time [?]. When the hand makes contact with different objects, distinct temperature curves are presented based on the physical properties of the objects and the hand. Various studies have been conducted to predict the extent of heat exchange between the hand and objects during this phenomenon, considering the physical properties. The study that generalizes the phenomenon of contact between objects and the hand is known as thermal modeling. This method analyzes the heat transfer process between objects and skin temperature, taking into account the physical factors. For short contact times, the most common interpretation of thermal models is based on the assumption of semi-infinite bodies' contact. A semi-infinite body refers to an idealized body with a single plane surface extending to infinity. When contact times are brief with shallow penetration depth, both the skin and the target object can be approximated as semi-infinite bodies. Generally, the semi-infinite body assumption is considered valid when the Fourier number (F_o) is less than 0.05.

$$F_o = \frac{\alpha t}{L_c^2}$$

The Fourier number is obtained by dividing the thermal diffusivity (α) and the contact period (t) by the characteristic length (L_c), which represents the length over which conduction occurs. Considering that sensors for perceiving the skin are distributed within 1-4 mm from the skin's surface, assuming an average of 2.5 mm, the semi-infinite body assumption is appropriate for contact durations up to 3 seconds [?]. A semi-infinite body assumes no thermal contact resistance between the two media. This model predicts that the skin and the object will maintain a constant temperature upon contact. This temperature is referred to as the Contact temperature T_c , and the formula for its calculation is as follows[?].

$$T_c = \frac{T_{object,i}(kpc)_{object}^{1/2} + T_{skin,i}(kpc)_{skin}^{1/2}}{(kpc)_{object}^{1/2} + (kpc)_{skin}^{1/2}}$$

$T_{object,i}$ is the initial temperature of the object, $T_{skin,i}$ is the initial temperature of the skin, and $(kpc)^{1/2}$ is called the contact coefficient. According to the equation, the T_c is maintained closer to materials with larger contact coefficient. However, when the actual skin of the hand contacts an object, there are typically tiny gaps that act as thermal resistances. Ho and Johns conducted research on a haptic display method using a model that accounts for thermal contact resistance in the semi-infinite model [?]. They proved that their approach created a more realistic model than previous methods. While this model can predict initial temperatures, it starts to differ from the actual data as the contact time increases. To better predict the skin temperature during the later phase of contact with the object, models considering metabolic heat generation and blood perfusion have been proposed [?, ?, ?, ?], There are also examples where the skin was divided and analyzed into multiple layers based on anatomical analysis [?, ?].

2.3 Thermal Haptic Devices in VR/AR

With the advancement of virtual reality technology, research is actively being conducted on methods to perceive the physical properties of objects beyond audio-visual sensations using wearable devices [?]. In the virtual environment, thermal haptic devices primarily takes the form of a glove. [?, ?, ?, ?]. Researchers have combined new thermal displays, thermal models, and form factors to improve previously challenging phenomena [?, ?, ?, ?, ?, ?, ?]. As touching an object during thermal rendering provides sudden haptic feedback, research has proposed devices utilizing preheated heat sources to represent this. Yatharth Singhal et al. use ultrasound sensors to apply pressure and combine them with preheated steam [?]. Shaoyu Cai et al. presented an air-based solution that employs preheated air chambers to represent temperature changes [?]. Sebastian Günther et al. suggested a method of preparing cold and hot water, mixing them, and using a water pump to provide thermal feedback [?]. However, these studies have the limitation of using materials with low thermal conductivity,

resulting in slow rates of raising or lowering the skin's surface temperature.

III. Peltier Actuator and Thermal Rendering

3.1 Peltier Actuator

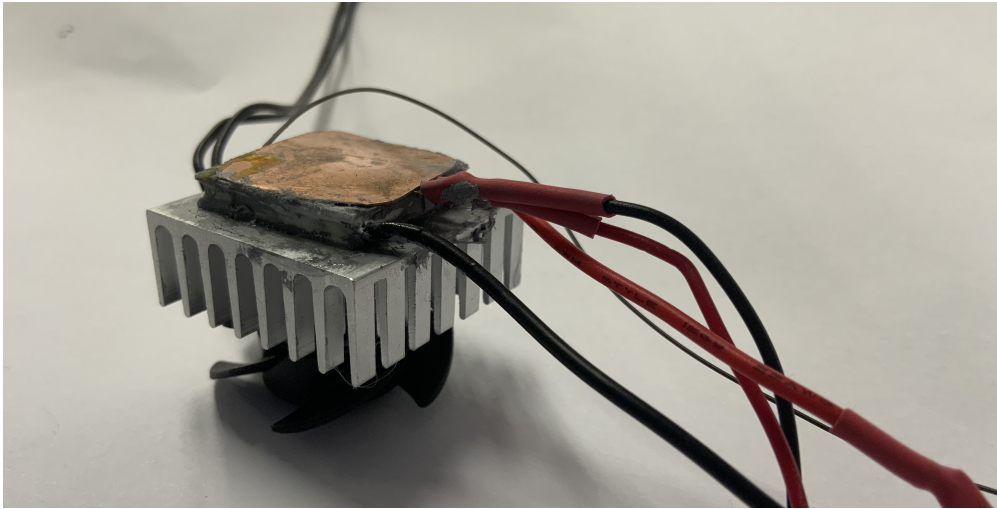


Figure 3.1: Peltier Actuator

A thermal display typically consists of a thermal simulator, thermal sensor, and temperature control system [?, ?, ?]. The most commonly used device for the thermal simulators is the Peltier device [?, ?, ?, ?, ?].

The Peltier device is a device that utilizes the Peltier effect, which occurs when two different metals are connected at two junctions. When a direct current voltage is applied to the two metal ends, electrons require a considerable amount of energy to move from one metal to the other with a potential difference. The Peltier effect exploits this phenomenon of extracting energy from the metal. Applying a direct current voltage to the two opposite sides of these different materials results in a phenomenon where one side absorbs heat, while the other side produces heat. Peltier devices have

advantages such as fast response time, low noise, and being smaller than other temperature simulators. The Peltier element has the advantage of a faster response time compared to other simulators, emits less noise, and can be manufactured in a relatively compact size. Efficient heat dissipation is crucial to maintaining the device's effectiveness. Common methods of heat dissipation involve attaching a heat sink to the back of the Peltier device and utilizing liquid cooling or air cooling methods. The maximum cooling rate of a commercial single Peltier device at room temperature is around 5 per second, and its heating rate is 13 . One proposed method to increase the maximum cooling and heating rates of the limited single Peltier device is to use a multi-stage Peltier module. This involves arranging the Peltier elements in a pyramid shape to enhance the operational efficiency of the top Peltier element. However, this method requires multiple Peltier elements, leading to higher energy consumption and a need for a more efficient cooling system. Other devices suitable for cooling simulators include vapor compression refrigerators or absorption refrigerators. Both methods have a higher COP (cooling capacity per unit power consumed) than the Peltier element. The downside is that they require a compressor and cooler and have a slower response time than the Peltier element.

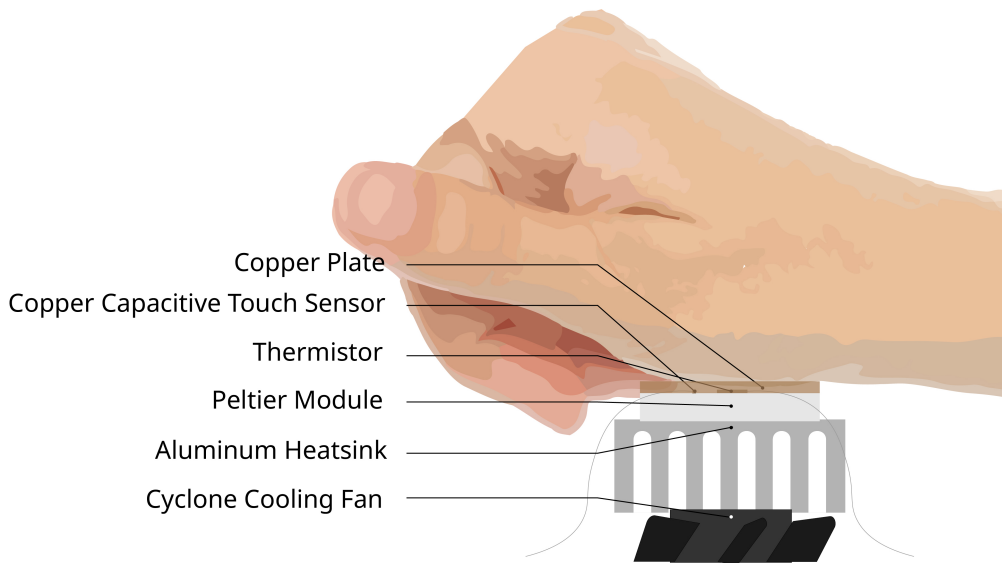


Figure 3.2: Structure of the Peltier Actuator

The simulator of the thermal display used in this paper is a Peltier module (Tec1-04903; 20x20mm). The embedded board (ESP32, Mbed) transmits target temperatures through serial communication. The temperature of the Peltier module is sensed in real-time at 1000 Hz using a thermistor (Ultra Thin 10K Thermistor - B3950, Adafruit; 3.8x25x0.4 mm). The embedded board employs PID control at 1000 Hz. The ESP32 compares the received target temperature from the PC with the current temperature difference and then sends a control signal to the DC motor driver (DRV8833, Pololu) by transmitting a PWM signal to adjust the voltage. The control loop operates at a frequency of 1000 Hz. To sense the surface temperature of the Peltier component, a thermistor is attached, along with thermal grease and a copper plate with a thickness of 0.2 mm. For sustained usability, the Peltier module is affixed to an aluminum heatsink, and cooling for the heatsink is facilitated by a Ball Bearing Cyclone cooling Fan (XR10 PRO G2S, Hobbywing; 30x30mm). The Cyclone Fan is supplied with approximately 3.7 V of voltage.

A graph for the Peltier device's cooling measurement data (from 60°C to 5°C) and heating measurement data (from 0°C to 55°C) is as shown in figure 3.3. Initially, there's a gentle start, which is due to low-pass filter. The heating rate increases as the temperature decreases, while the cooling rate increases as the temperature rises. The efficiency of the heating rate and cooling rate is determined based on the temperature on the opposite side of the Peltier device. This device uses an air-cooling method, so the temperature on the other side is similar to the room temperature. Overall, the heating rate is faster than the cooling rate.

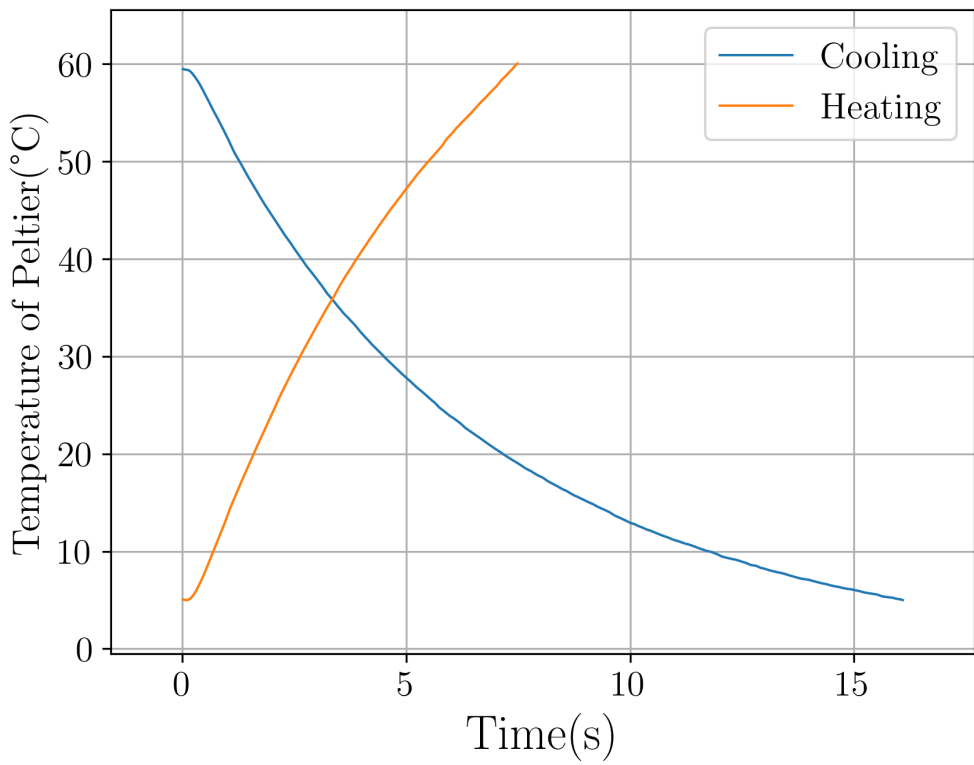


Figure 3.3: Temperature Measurement Results During Cooling and Heat Dissipation of the Peltier Actuator

3.2 Thermal Rendering

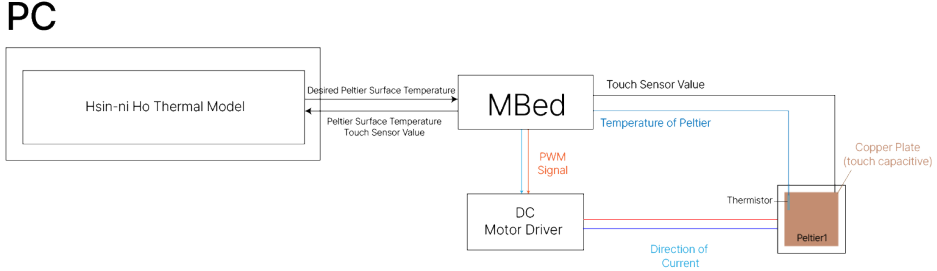


Figure 3.4: An Overview of Thermal Rendering Using the Peltier Actuator

The system adjusts the temperature of the thermal display following Ho and Johns' thermal model [?]. Here, k_{object} represents the thermal conductivity of the object in contact with the skin. Simulation results, which incorporate the thermal resistance between the objects, demonstrate improved initial predictive accuracy compared to a semi-infinite body model. The temperature representation predicted by the modified differential equation, considering these resistances, can be analyzed as follows:

$$T_{skin,s}(t) = \frac{A}{B} \{1 - e^{\alpha_{skin} B^2 t} \operatorname{erfc}[B(\alpha_{skin} t)^{1/2}]\} + T_{skin,i}$$

$$A = \frac{-(T_{skin,i} - T_{object,i})}{\kappa_{skin} R}, B = \frac{1}{\kappa_{skin} R} \left[1 + \frac{(kpc)_{skin}^{1/2}}{(kpc)_{object}^{1/2}}\right]$$

$$T_{object,s}(t) = \frac{C}{D} \{1 - e^{\alpha_{object} D^2 t} \operatorname{erfc}[D(\alpha_{object} t)^{1/2}]\} + T_{object,i}$$

$$C = \frac{(T_{skin,i} - T_{object,i})}{\kappa_{skin} R}, D = \frac{1}{\kappa_{object} R} \left[1 + \frac{(kpc)_{object}^{1/2}}{(kpc)_{skin}^{1/2}}\right]$$

The thermal interaction model includes skin surface temperature, object surface temperature, and heat flux during contact. where T is the temperature, α is the thermal diffusivity, κ is the thermal conductivity, R is the thermal contact resistances, ρ is the density, t is time, c is the specific heat. $\text{erfc}()$ is the complimentary error function. Subscripts i and s mean the initial and surface temperature, respectively. The $R_{skin-display}$ represents the resistance between each haptic display and the skin.

According to Ho and Johns' model, based on the thermal display's surface temperature, the thermal resistance between the thermal display and the skin, and the initial skin temperature conditions, one can determine the temperature conditions that the thermal display should meet over time.

A haptic display that makes contact with the hand and can control surface temperature over time. The skin temperature on hands and feet, being farther from the heart, is lower than the overall average, with a typical hand skin temperature known to be 34 . The thermal resistance between a solid material made using a milling machine and the skin is reported to satisfy the following conditions. The thermal contact resistance when in contact with objects that have undergone similar surface treatments produced by a milling machine and applying a force of 2 N is known to follow the following equation:

$$R_{skin-object} = \frac{0.37 + \kappa_{object}}{1870 \cdot \kappa_{object}} (m^2 K/W)$$

Based on the Ho and Johns model, the initial temperature of the thermal display is adjusted by applying it as a parameter of thermal rendering when contacting the skin in a virtual environment. Here, the initial temperature of the hand is assumed to be 34 for calculations. When an object and the hand touch, the skin temperature of the hand and the surface temperature of the object are calculated and the target temperature value for the display is transmitted via serial communication. The thermal display strives to match this value as closely as possible. The calculation frequency is 1000 Hz, and when contact is lost, the surface temperature of the skin on the hand is assumed to be 34 . Peltier devices are made of Alumina Oxide material. In this study, the thermal

conductivity of peltier actuator is $18\text{K/w}\cdot\text{m}$. The surface temperature of the previously mentioned thermal display is specified by above resistance equation. For instance, if the nearest object is made of Granite material with a temperature set to 13 (Thermal Conductivity: $3.1\text{ (W/(m}\cdot\text{K))}$, Density: $2700\text{ (kg}\cdot\text{/m}^3\text{)}$, Specific Heat: 790 (J/kg)), the target temperature is 9.3831 . A characteristic of the HoJohns model is that over time, the temperature of the thermal display and the skin converges to the contact temperature. When using this model, it is important to note that it does not reflect factors such as heat propagation due to blood flow and the heat effect caused by cell metabolism. Such issues cause discrepancies between the model and actual results as the contact time progresses. Below are the target profiles and actual rendering results when touching objects at temperatures of 8 , 22 , 40 , and 55 , respectively, for Aluminum, Granite, Glass, and Acrylic.

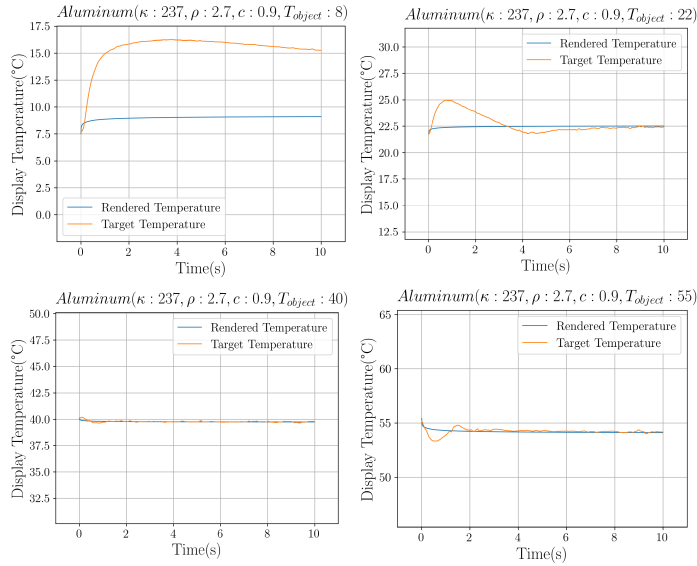


Figure 3.5: Temperature rendering results for aluminum with different target temperatures

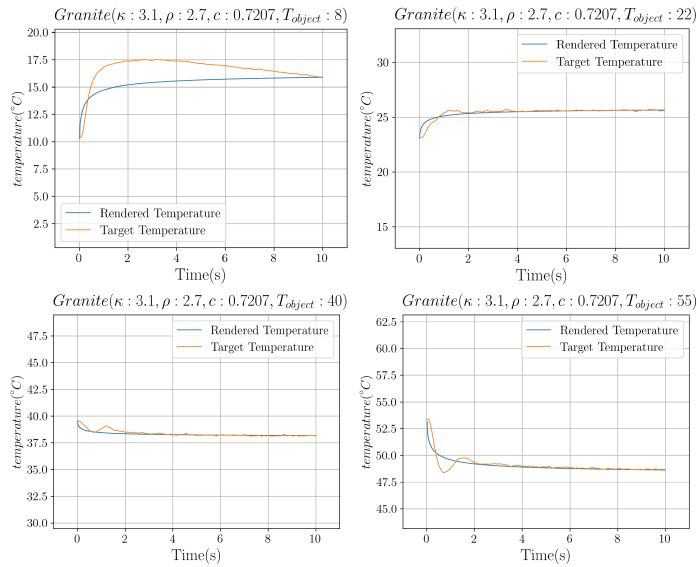


Figure 3.6: Temperature rendering results for granite with different target temperatures

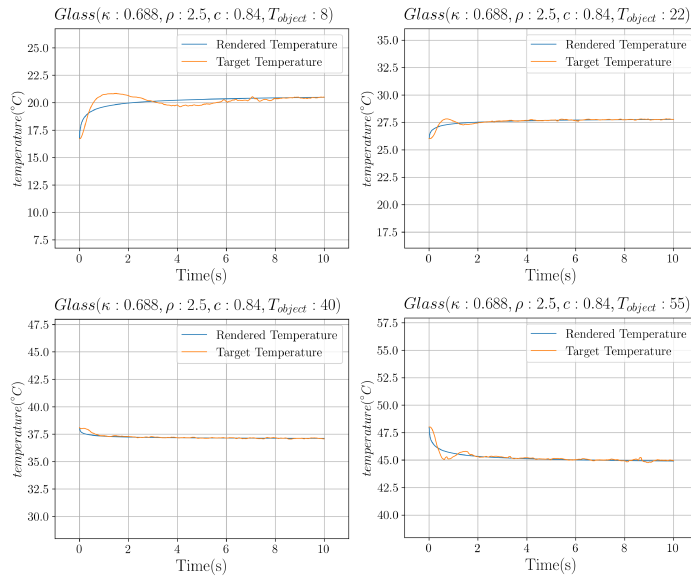


Figure 3.7: Temperature rendering results for glass with different target temperatures

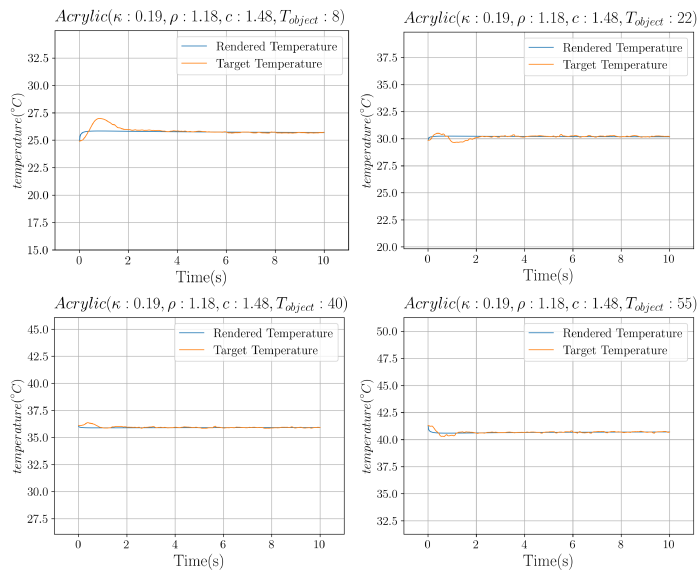


Figure 3.8: Temperature rendering results for acrylic with different target temperatures

The rendering results show several common characteristics:

1. The greater the difference between the skin's temperature and the target temperature, the greater the difference from the target rendering curve.
2. Peltier devices have a lower efficiency for temperature decrease compared to temperature increase. Thus, for the same temperature difference, rendering for a lower temperature differs more than rendering for a higher temperature.
3. At the initial contact, there is a significant difference from the target curve, but over time, they tend to match.

Depending on the performance of the display and the material in contact, there's a range in which the rendering curve can be presented similarly. Therefore, users aiming for realistic temperature rendering should check whether the combination of display performance, material, and temperature can provide the appropriate rendering.

3.3 Simulation

Creating environments for individual experiments to estimate the limits of what the thermal display can express can lead to uncertainties and high costs. Simulation programs can reduce these costs and time. Additionally, the simulation program can help analyze the surface temperature inside the skin, compare with other temperature displays, or predict effects during improvements.

3.3.1 Implementation

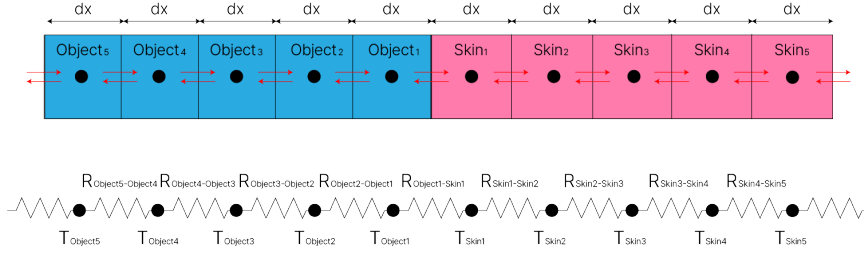


Figure 3.9: Temperature rendering results for glass with different target temperatures

We implemented a simulation program following the Finite Difference Method (FDM) for the non-steady-state heat conduction equation of a one-dimensional structure, based on Ho and Johns' model. The simulation assumed a one-dimensional non-steady state heat conduction scenario. The time updated at every frame was assumed to be dt , and the length of one unit segmenting the object was assumed to be dx .

$$R_{skin(m)-skin(m+1)} = \frac{dx}{\kappa_{skin} \cdot A}$$

$$R_{object(n)-skin(n+1)} = \frac{dx}{\kappa_{object} \cdot A}$$

$$R_{object-skin} = \frac{0.37 + \kappa_{object}}{1870 \cdot \kappa_{object} \cdot A}$$

$$R_{object(1)-skin(1)} = \frac{dx/2}{\kappa_{object}} + \frac{dx/2}{\kappa_{skin}} + R_{object-skin}$$

$$q''_{skin(m)-skin(m+1)} = \frac{-(T_{skin(m)} - T_{skin(m+1)})}{R_{skin(m)-skin(m+1)}}$$

$$q''_{object(n)-object(n+1)} = \frac{-(T_{object(n)} - T_{object(n+1)})}{R_{object(n)-object(n+1)}}$$

$$q''_{object(1)-skin(1)} = \frac{-(T_{object(1)} - T_{skin(1)})}{R_{object(1)-object(1)}}$$

$$dT = \frac{(q''_{left}(t) + q''_{right}(t)) \cdot dt}{C(A * dx)\rho}$$

3.3.2 Comparison with Ho's Model

The following graphs compare the results of the Semi-infinite model considering thermal resistance by Hsin-ni Ho with those of the Finite Element Analysis developed by incorporating Ho's thermal resistance properties. The initial conditions are such that one iteration time is 0.00002s, and the distance between each element is 0.0001m.

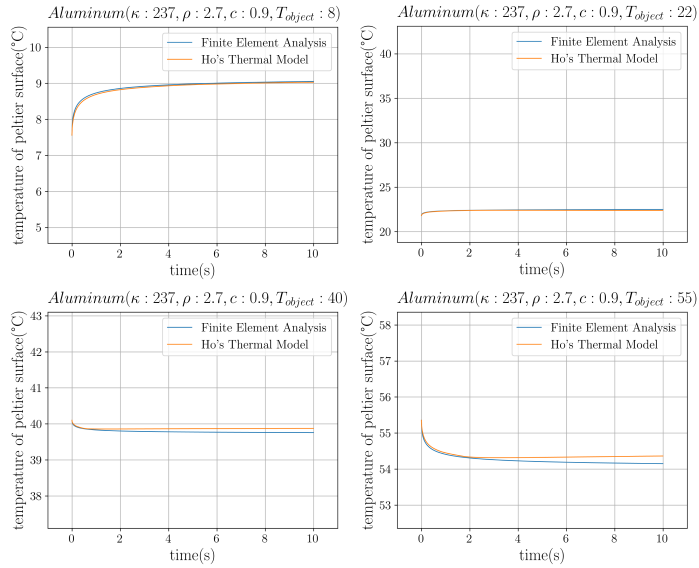


Figure 3.10: Finite element analysis results for aluminum with different temperatures

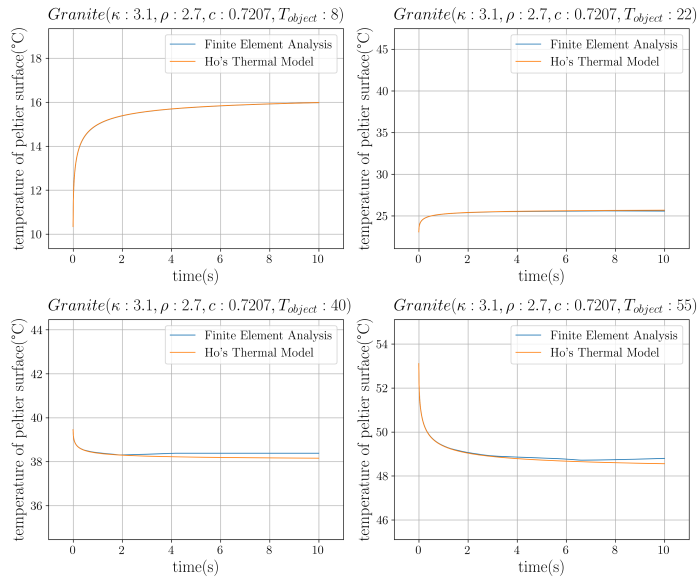


Figure 3.11: Finite element analysis results for granite with different temperatures

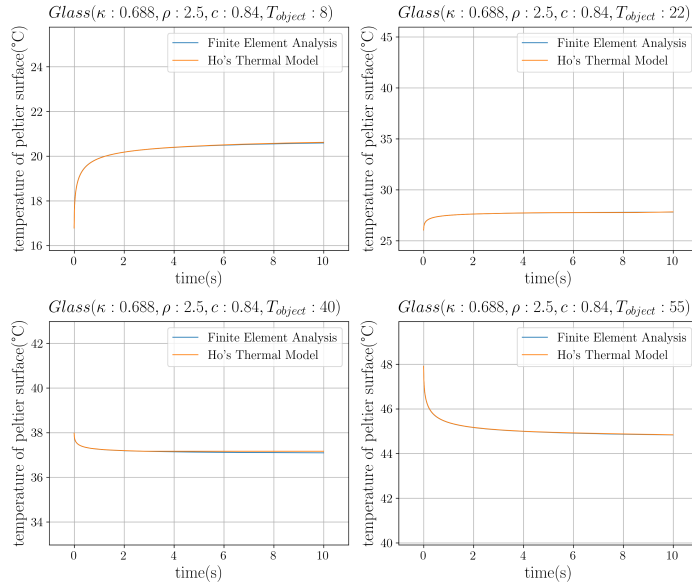


Figure 3.12: Finite element analysis results for glass with different temperatures

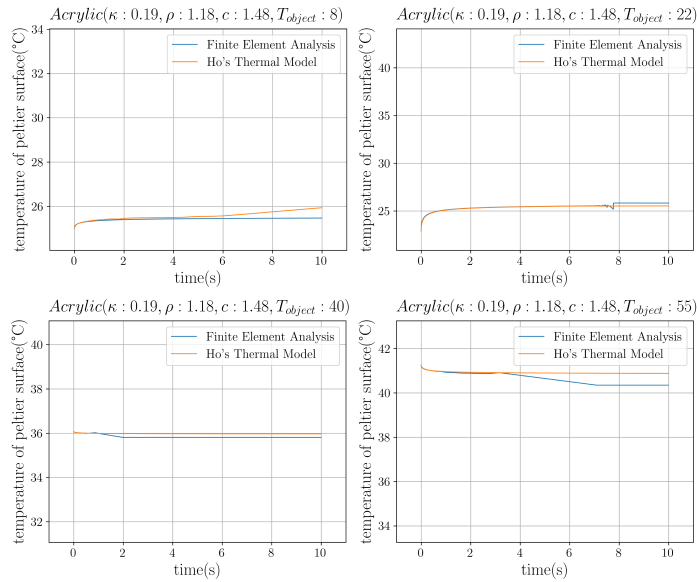


Figure 3.13: Finite element analysis results for acrylic with different temperatures

3.3.3 Comparison with Measured Data

The results of the simulation model and the measured rendering method are as follows. In each graph, the green line represents the predicted graph for the Peltier display, the orange line represents the actual measured temperature of the display, and the blue line represents the target temperature curve.

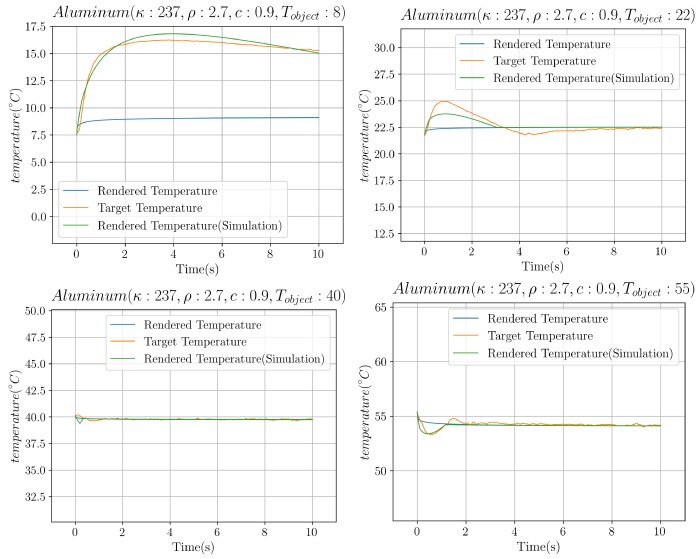


Figure 3.14: Simulation results for aluminum with different temperatures

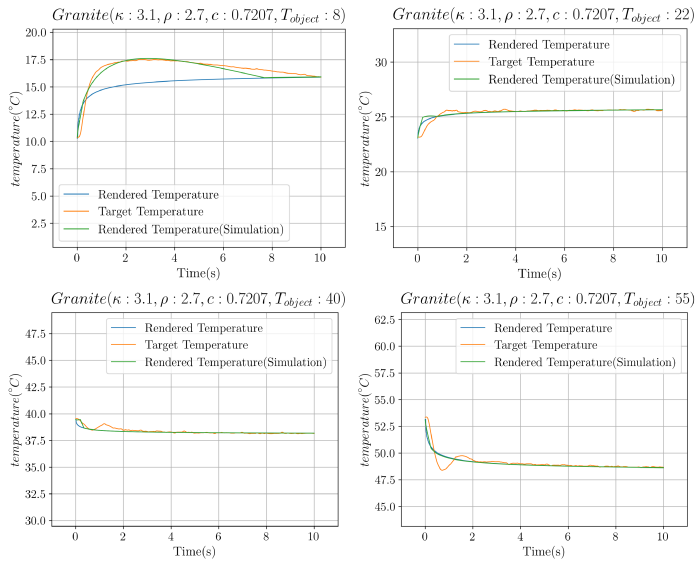


Figure 3.15: Simulation results for granite with different temperatures

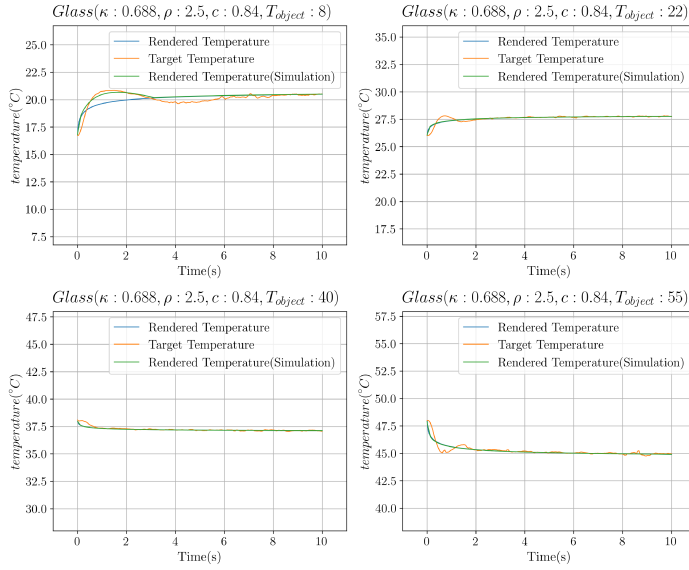


Figure 3.16: Simulation results for glass with different temperatures

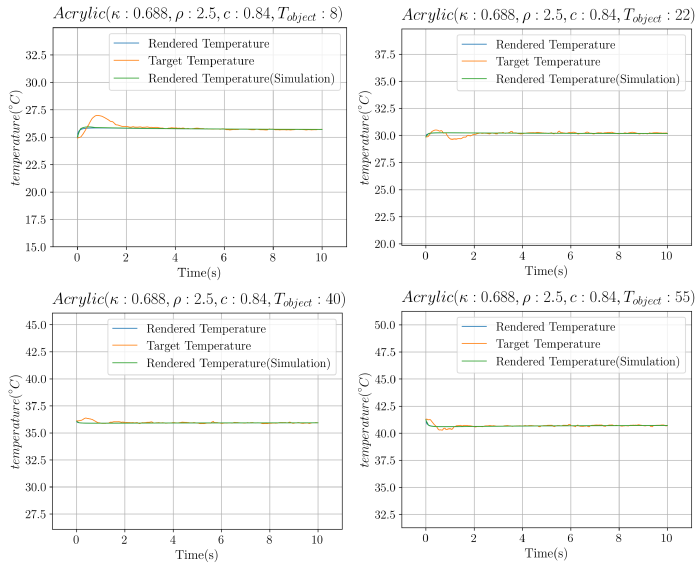


Figure 3.17: Simulation results for acrylic with different temperatures

As can be seen in the figure, the predicted graph and the actual results are similar. Through the simulation program, users can quantify the medium and display performance to predict the results. The predicted graph when the Peltier device's heating and cooling rate are doubled is Figure 3.15. We can confirm from the simulation results that the error relative to the target curve has been reduced.

3.3.4 Utilization of the Simulation

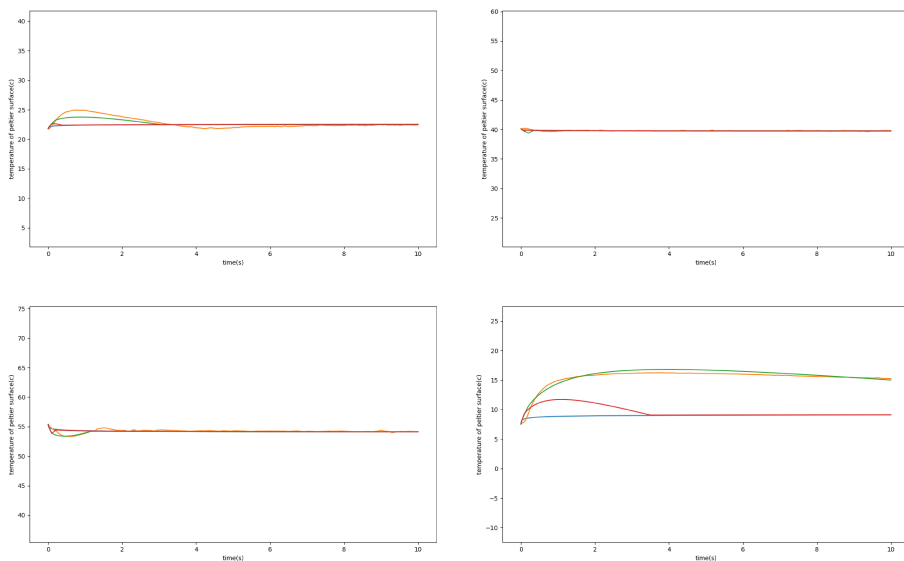


Figure 3.18: Temperature Simulation Results for Aluminum with Varying Temperatures Using a Peltier Actuator with a Cooling Rate Twice as Fast

The rendering method presented to be more similar to the target curve might be perceived differently by the user. Through this simulation program, we utilized it to compare a single material that can provide thermal changes similar to the feeling of touching an object where two or more materials, such as a wine bottle made of glass and an aluminum can filled with cola, are arranged in combination, and to predict temperature rendering results according to the performance of a new display.

IV. Multiple Rotating Pre-heated Peltier Actuators

4.1 Hardware Implementation

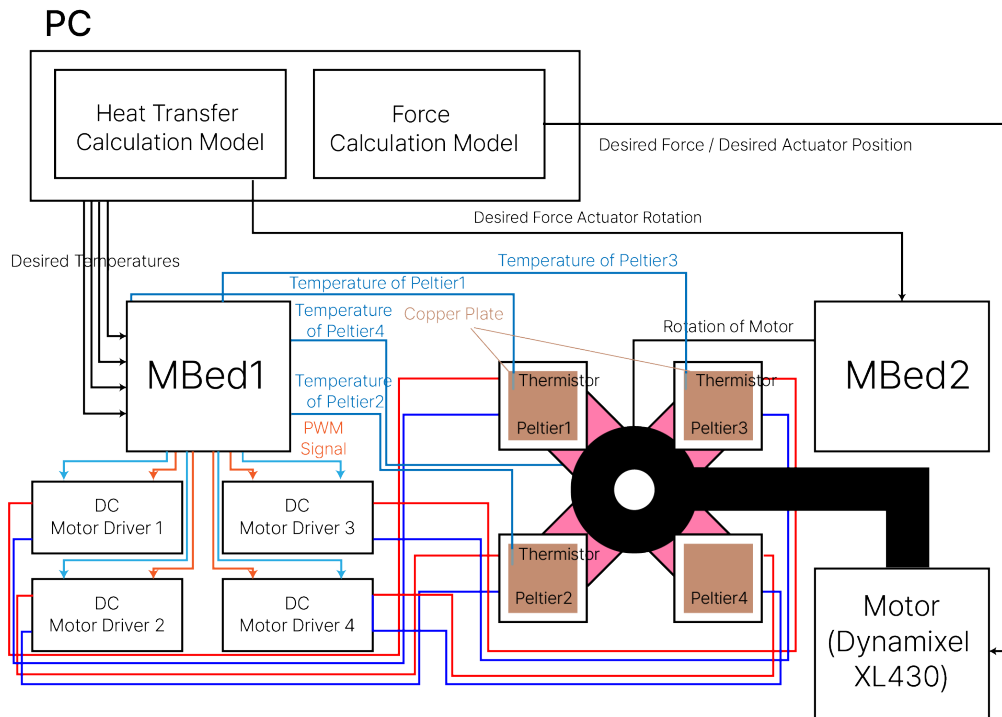


Figure 4.1: System diagram of multiple rotating pre-heated Peltier actuators

The system overview is summarized as Fig. 4.1. Our system use a game engine (Unity) to detect interactions with virtual objects through the computer and provide users with force and thermal feedback. The haptic feedback provided to the user is focused on the palm of the hand. On the PC side, collision result values and target

temperature values are calculated to determine the haptic effects to be provided to the user. For the force feedback, device operates at a frequency of 1000 Hz. Users wear the Meta Quest HMD and utilize the hand tracking feature provided by Meta to determine the position of their hands. In Unity, objects within 30 cm of the palm surface are detected, and preheating commands for the temperature of the closest object are given to the Peltier actuators. When a collision is detected, a command for contact between the device and the palm is provided, and the user receives thermal feedback when the device touches their hand. When the user grasps the touch sensor, a grab command is activated, assuming that the user is holding the object, and they receive force feedback related to the object. Two servo motors were employed to provide thermal feedback (one camera is positioned beside the wrist and the other is attached next to the pedestal). The motor beside the wrist operates at a voltage of 12 V, while the other motor operates on a 3.7V single-cell battery.

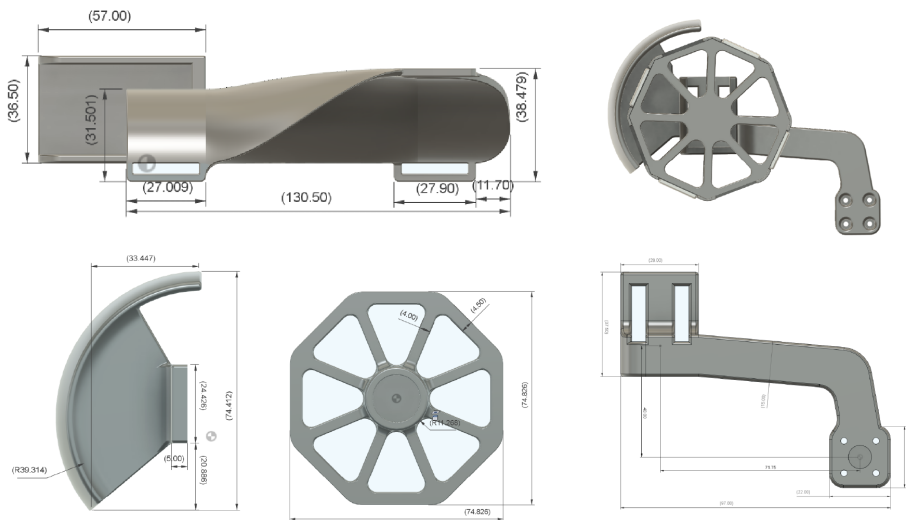


Figure 4.2: Dimension of the device components

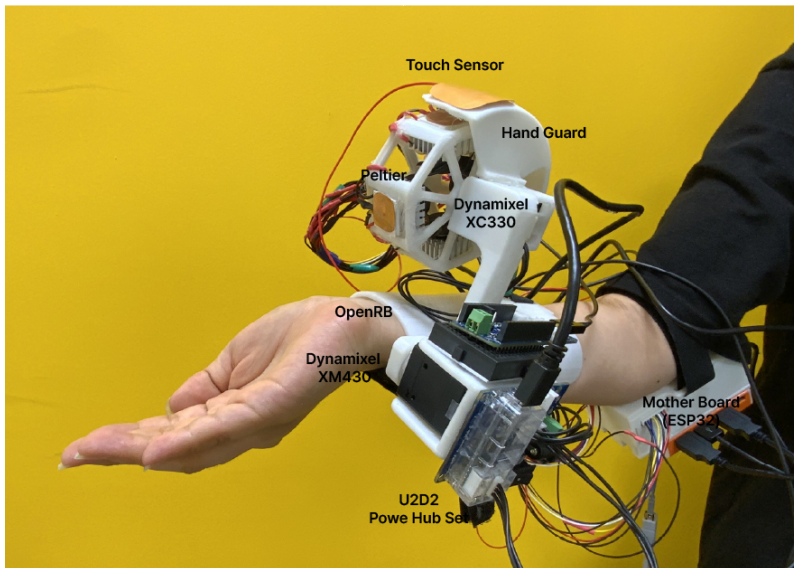


Figure 4.3: Appearance of the wearable Hardware

4.2 Software Implementation

4.2.1 Lumped System

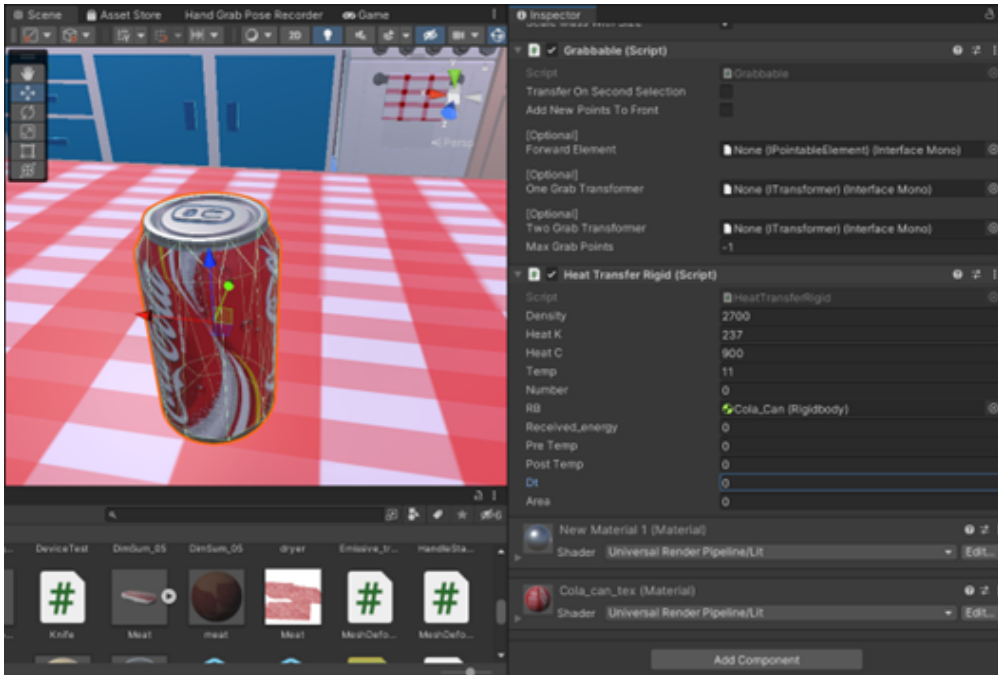


Figure 4.4: Temperature Parameter Setting Screen in Unity Program

Thermal rendering in VR environments differs from FEM (Finite element method) in that it requires real-time computation and immediate reflection of the results. Objects during contact are represented as concentrated capacitors and computed accordingly. In this system, objects in the virtual space are analyzed using lumped system analysis. If the temperature gradient within a solid is negligible, the entire solid can be represented by a single representative temperature. In thermal analysis, there are cases where the internal temperature of an object remains constant at a certain time. Concentration field analysis assumes that the overall temperature of the object is constant and the conductive thermal resistance within the object is assumed to be zero[?].

The lumped system analysis is a simple and convenient approach that can be used

to solve transient heat conduction problems. The reasonable accuracy of this method is typically verified through dimensionless parameters, known as the Biot Number, which represents the scale of temperature gradients within the solid compared to the temperature difference between the surface and the fluid. When the Biot Number is much smaller than the convective resistance at the fluid boundary, it is reasonable to assume that the temperature distribution is uniform. The Biot Number is known to be used when its value is less than 0.1. In the case of heat convection phenomena in a virtual space, as the thermal resistance approaches infinity, the Biot Number becomes zero, making this assumption reasonable. In Unity, user can set the specific heat, thermal conductivity, and density of each object.

4.2.2 Thermal Analysis of Objects Composed of Composite Materials

Wine glasses and water bottles typically have a form where they contain liquid inside and are encased in another material on the outside. The two substances have distinct properties. For instance, the simulation results for a wine glass filled with wine of 1 mm thickness, contact with a solid having the same thermal conductivity as water, a composite object differs from the combination of the two substances and varies by thickness. we substituted it with a new material that provides a graph similar to the given simulation.

4.3 Use Scenario

4.3.1 Preparing for Collision

Each Peltier element is assigned a reference temperature and a designated range. When the PC detects an anticipated contact object, it operates by changing from the reference temperature to the target temperature. If the PC does not detect an anticipated contact object, the four Peltier elements maintain their respective default temperatures as the target temperature.

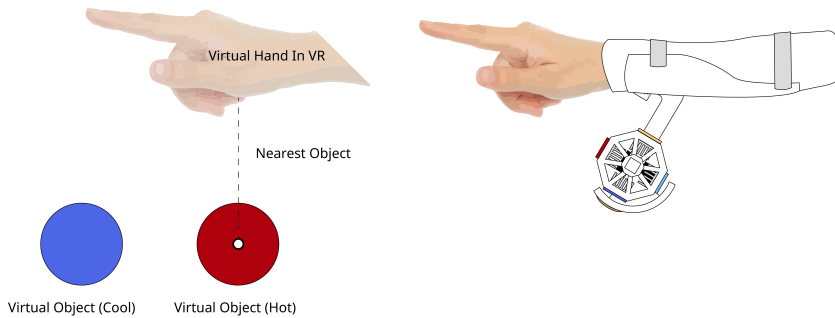


Figure 4.5: Appearance of the Multiple Rotating Pre-heated Peltier Actuators Depending on the Position of the Virtual Hand and Object in the Virtual Environment

The Peltier elements are arranged in a manner to minimize the maximum delay time taken to reach the target temperature within the given temperature range. Before

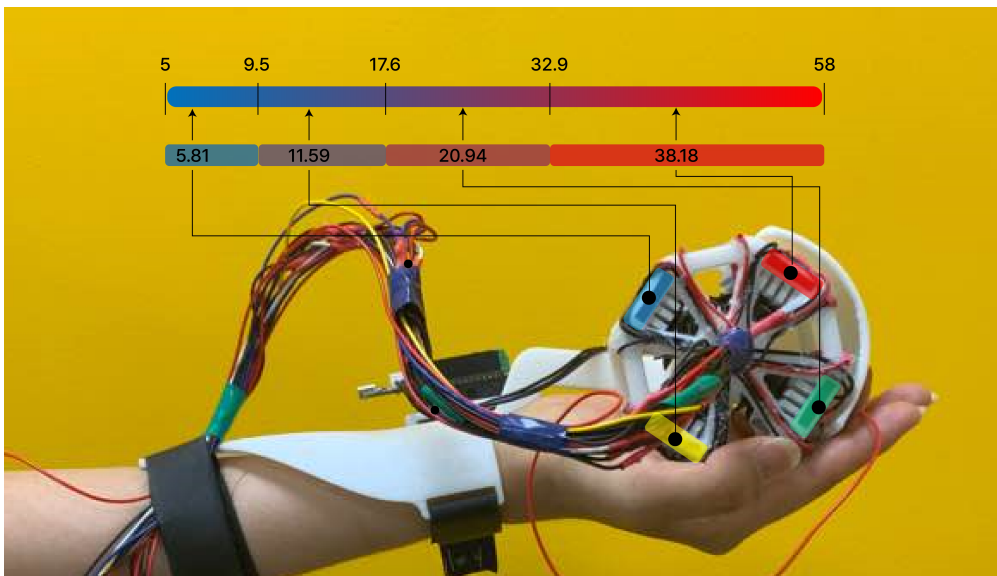


Figure 4.6: Temperature range and reference temperature of each Peltier in the multiple rotating pre-heated Peltier actuators

an object makes contact, to synchronize the initial temperature at the time of contact, this system assumes the object closest to the user within 30cm is the most likely object the user will come into contact with and synchronizes with its temperature. If there's no object within 30cm, all four Peltier elements maintain their initial temperatures.

Depending on which range the target temperature falls into, the contacting Peltier element is determined. Then, the PC, through the Mbed (Openrb-150, Robotis), controls the rotation via the Coreless DC Motor (XC330-M181, Robotis) so that the Peltier element responsible for the targeted range can touch the user's palm. The motor's rotation speed can turn at a rate of 2 rotations per second. Considering the situation where the four Peltier elements are equally distributed over 360 degrees, it takes approximately 0.25 seconds to rotate to an adjacent Peltier element and 0.5 seconds to rotate to the opposite Peltier element.

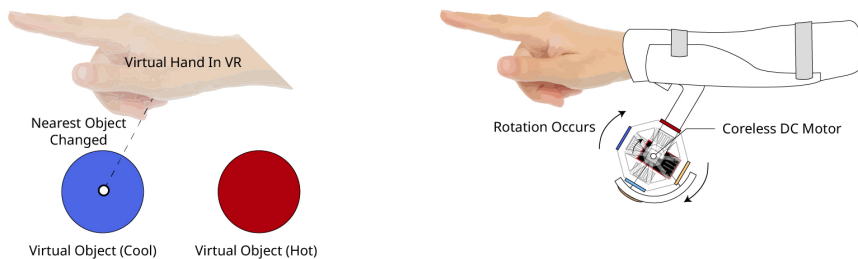


Figure 4.7: Appearance When the Closest Material Changes

4.3.2 Controlling Haptic Effects During Contact

When a collision with an object occurs in the virtual space, the rotating part moves through the Dynamixel XM430 motor to make contact with the hand. Since the Dynamixel XM430 can track current, the torque strength can be adjusted, allowing control over the pressure applied to the Palm area. Each of the four Peltier devices

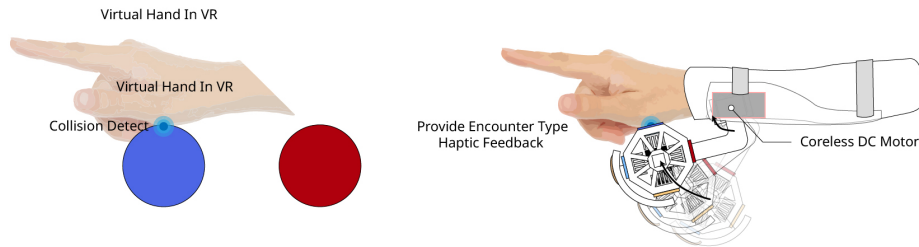


Figure 4.8: Appearance When the Virtual Hand Touches the Virtual Object

is connected to a copper plate with wiring to allow for capacitive Peltier sensing. The temperature rendering uses the time when the contact with the object started as a variable, and the contact time is recorded the moment the user and the Peltier device touch. The contact time is used as an input parameter to calculate the target temperature of the thermal display, which in turn renders the temperature of the virtual object.

4.3.3 Grasping and Releasing Object

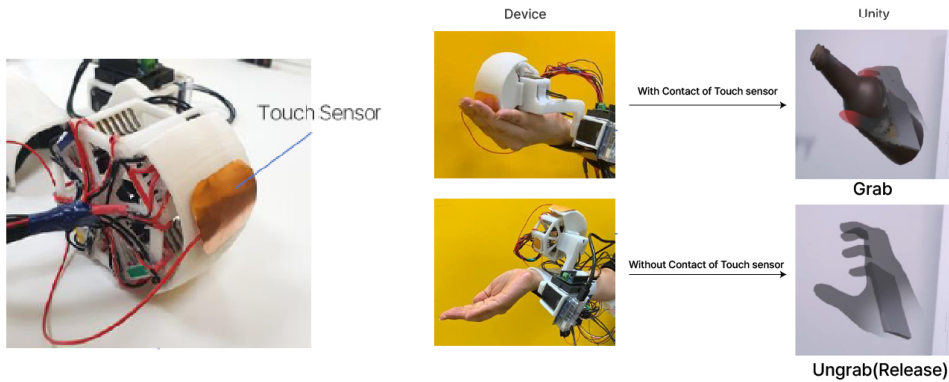


Figure 4.9: Example of Grasp and Ungrasp Operation Depending on the Contact of the Touch Sensor

A copper-based patch is placed at the bottom of the guard to prevent fingers from touching the target Peltier device. The touch sensor's contact status in the guard section changes the Grip/Ungrasp settings. When the hand wraps around the touch sensor, the avatar in the virtual space grabs an object with the pose registered through the pose registration feature in Unity Meta SDK. When holding an object, weight rendering is applied in real-time, with the vertical resistance changing based on the palm's angle and the direction of gravity. When the touch sensor is released, the pose is deactivated, and the weight rendering application is canceled.

V. User Experiments

In this evaluation experiment, we conducted a study to determine whether there is a perceptual difference in the condition that allows users to rapidly adjust the initial temperature conditions when they come into contact with virtual objects in a simulated environment, using multiple pedestal devices compared to using a single pedestal device, and whether this could have an overall positive impact on the user experience. The experiment was conducted under the protocols approved by the Institutional Review Board at the Postech(PIRB-2023-E007).

5.1 Methods

5.1.1 Participants

A total of 12 participants took part in this experiment(7 female and 5 male, ages 20 to 29, average 23.83). None of the participants reported any issues with perceiving thermal sensations. The experiment took an average of 45 minutes, and the participants were compensated with 15,000 KRW after completing the study.

5.1.2 Experimental Conditions

Two demo VR scenarios were presented, each containing examples of thermal haptic feedback. The Meta Quest Pro was used as the VR HMD, and the hand tracking method utilized the Meta Quest's own hand tracking system. The setup is designed to provide an abrupt thermal conduction effect, with experiment scene 1 featuring objects of the same properties but different temperatures, while experiment scene 2 allows for the arrangement of objects with various properties and different temperatures. Users compare the experience for the above two scenarios using two different algorithms

(“With rotation” / “Without rotation”). Users can experience different thermal variations, providing insights into their unique user experiences regarding heat perception. Users can freely move their hand to touch the object. When a touch command occurs in the virtual environment, the device transmits the temperature curve to be provided based on the time the user’s hand made contact.

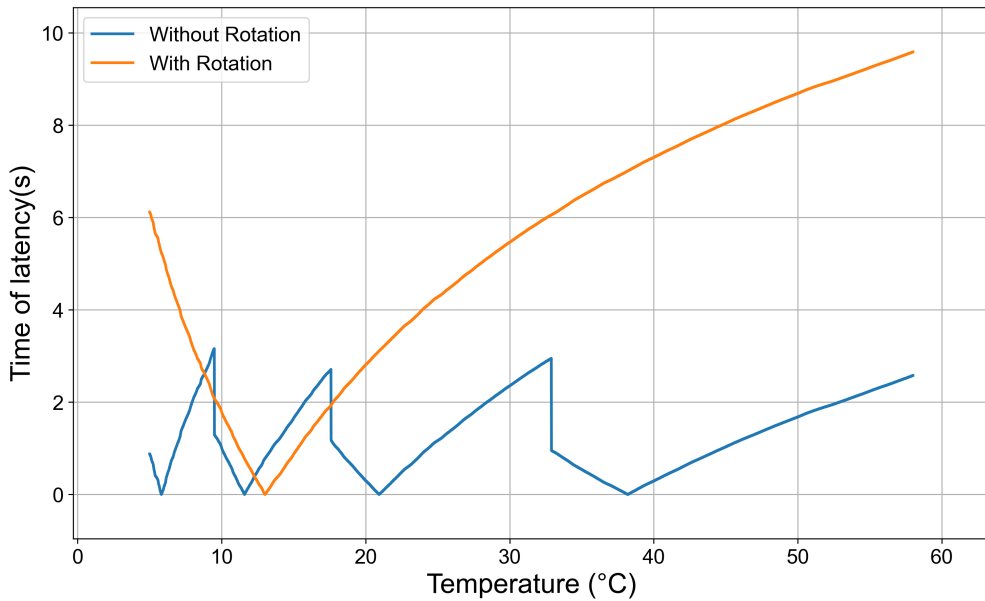


Figure 5.1: Comparison of Latency Time Based on Temperature for Two Algorithms

the 'With Rotation' algorithm takes an average of 1.27 seconds to match the initial temperature of objects ranging from 5 to 58 degrees Celsius, while the 'Without Rotation' algorithm takes 5.5 seconds.

Scenario 1 : Granite Stones

In this scenario, users freely experience touching Granite Stones that look the same but have different temperatures. Detailed settings for each initial temperature are presented as shown in the Fig 5.3. Users were allowed to freely touch objects and experience the temperature of the object. For Force Feedback, it is limited upon



Figure 5.2: Scenario 1 : Granite Stones

contact with the hand and only provides the sensation of the hand pressing with a constant torque; other force rendering methods were excluded.

Parameter Setting

Object	Thermal Conductivity W/(m·K)	Density kg/m ³	Specific Heat Capacity J/kg·°C	Initial Object Temperature °C	Initial Display Temperature °C
Granite Stone	3.1	2700	720.7	8	10.29
Granite Stone	3.1	2700	720.7	22	23.06
Granite Stone	3.1	2700	720.7	55	53.15

Figure 5.3: Scene1 thermal stimulus

Thermal Stimuli The graph of the target temperature curve starting from the initial temperature for each parameter and the result rendered on the haptic display is as follows.

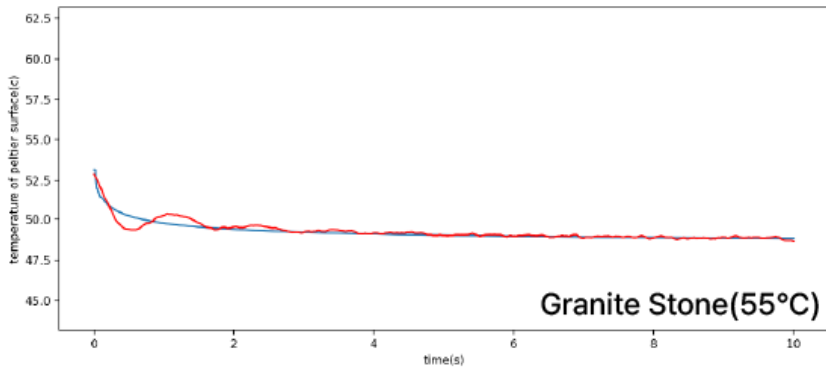
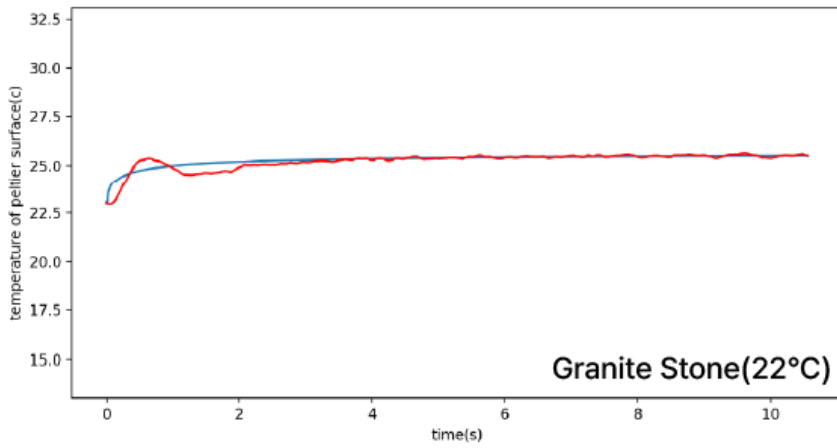
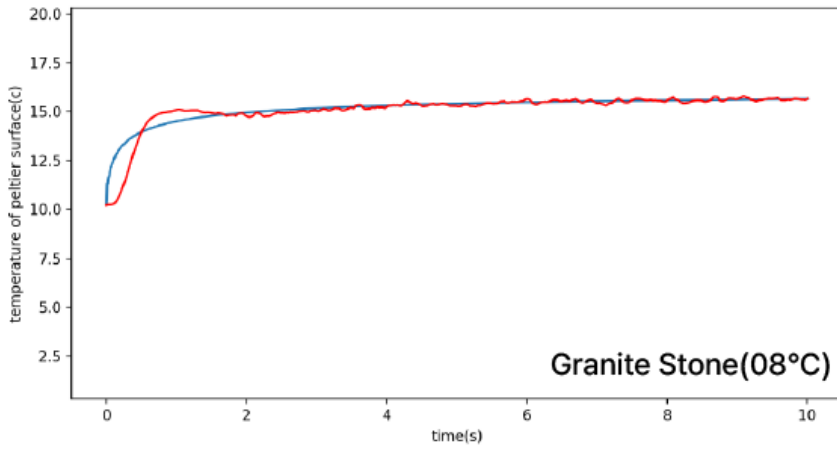


Figure 5.4: Thermal rendering results of granite stones

Scenario 2 : Dining Table



Figure 5.5: Scenario 2 : Dining Table

Measurement of thermal conduction experience within a virtual environment involving everyday actions. Users can interact with a variety of objects at different temperatures, picking them up, releasing them, and moving them around

Thermal Stimuli The graph of the target temperature curve starting from the initial temperature for each parameter and the result rendered on the haptic display is as follows.

Object	Thermal Conductivity W/(m·K)	Density kg/m ³	Specific Heat Capctly J/kg·°C	Initial Object Temperature °C	Initial Display Temperature °C
Kimchi Soup	12.5	1000	4189	55	54.81
Mug Cup	7	1000	4189	22	22.37
Steak	0.37	1250	3300	50	42.16
Wine Glass	0.5	1000	4189	5	16.99
Beer Can	1.6	1000	4189	5	9.96
Coke Can	1.6	1000	4189	10	14.11
Water Bottle	0.45	1000	4189	22	27.28
Wine Bottle	0.45	1000	4189	15	23.56
Spoon and Chopsticks	61	7833	460	22	21.83
Riceball	0.543	850	3000	44	40.07
Dumpling	0.41	1037	3440	54	44.73

Figure 5.6: Scene2 Stimuli

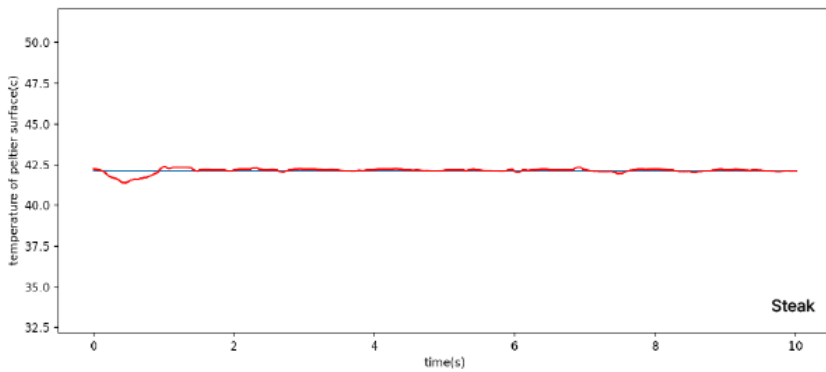
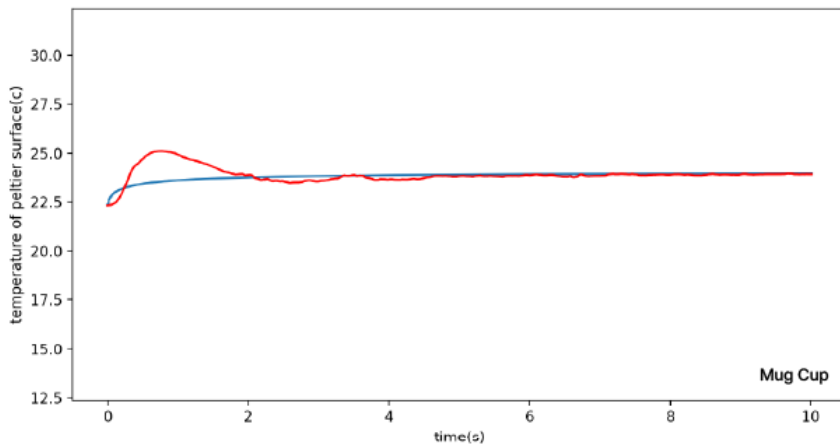
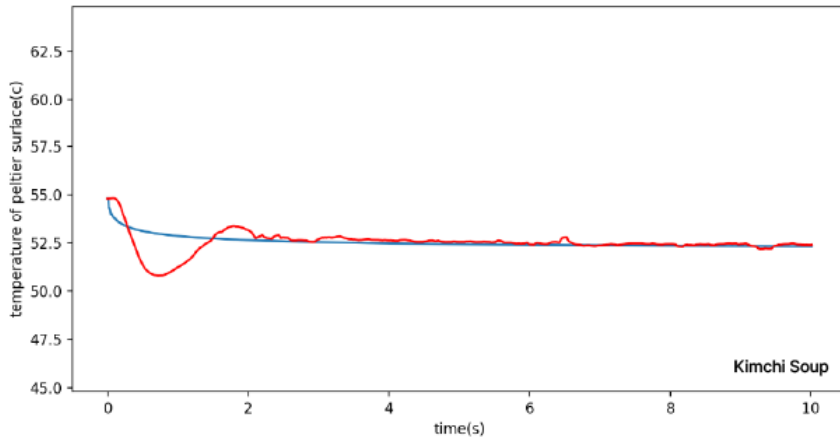


Figure 5.7: Thermal rendering results of kimchi soup, mug cup and steak

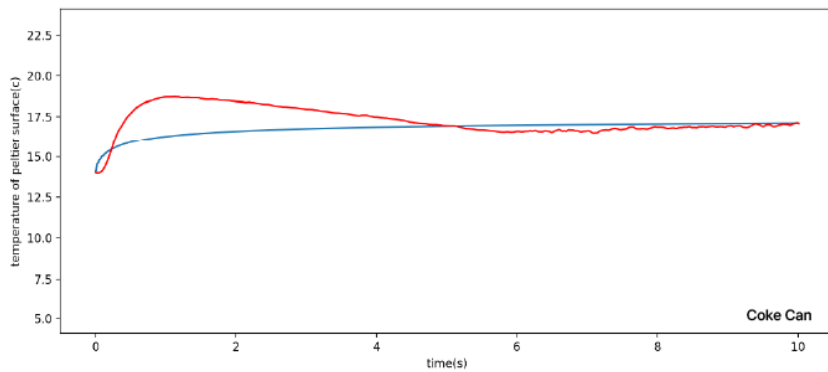
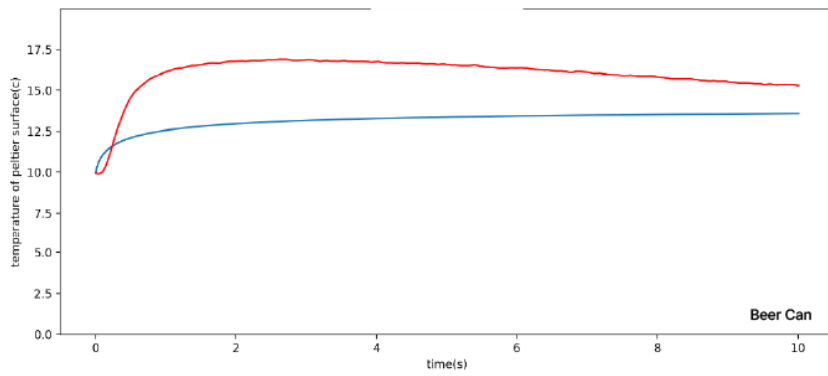
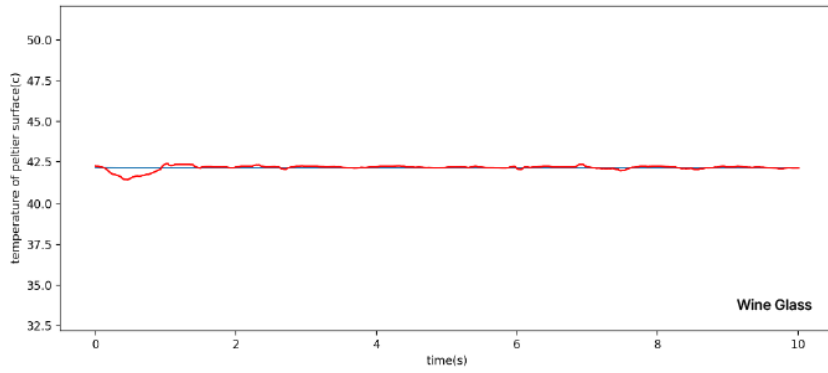


Figure 5.8: Thermal rendering results of wine glass, beer can and coke can

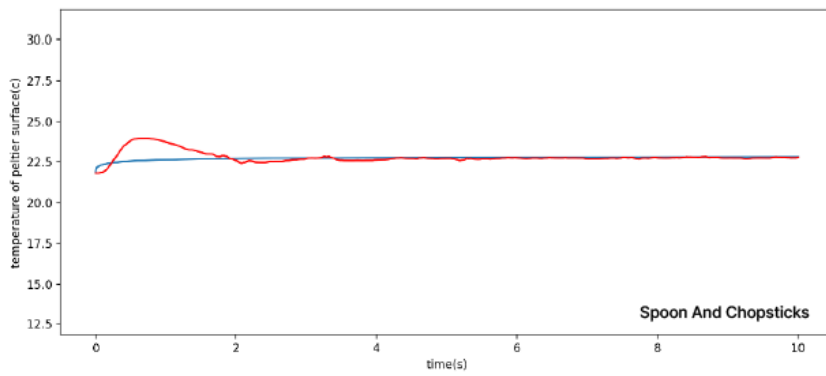
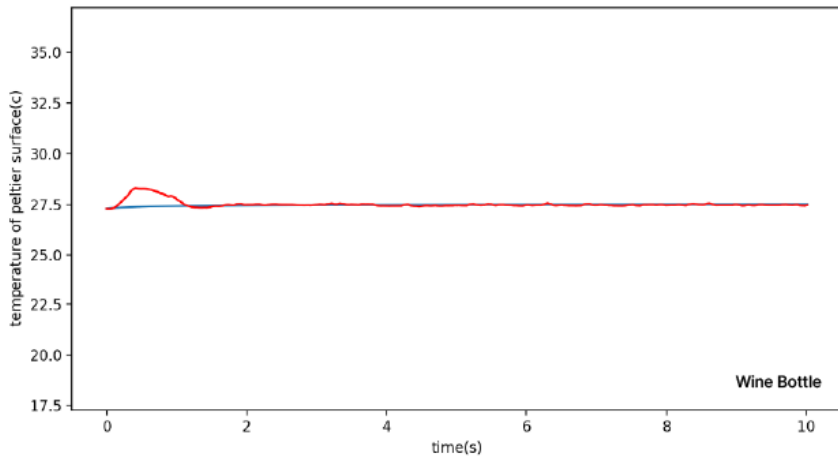
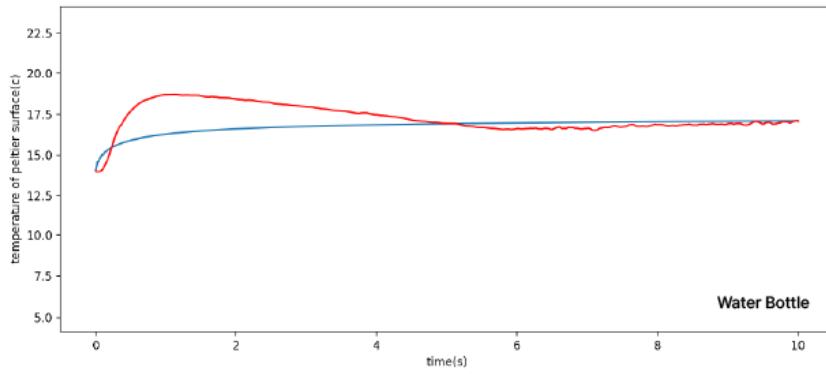


Figure 5.9: Thermal rendering results of water bottle, wine bottle, spoon and chopsticks

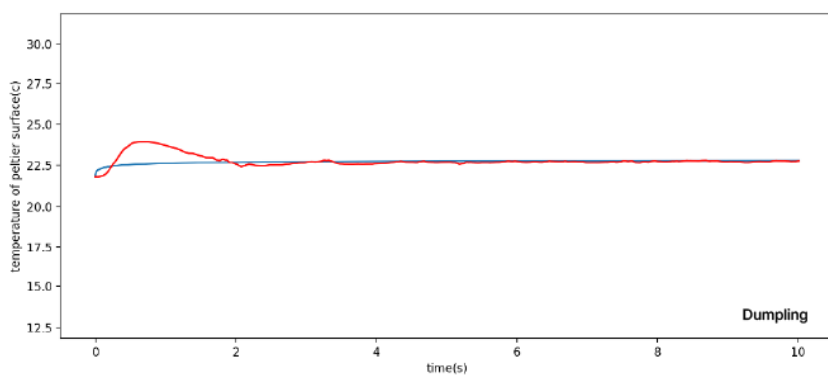
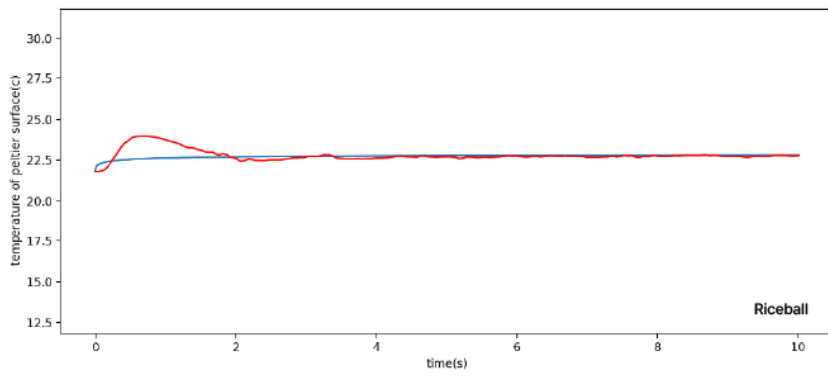


Figure 5.10: Thermal rendering results of riceball and dumpling

5.1.3 Evaluation

To assess the user's experience with the device, the following criteria were used for evaluation: Realism: The haptic feedback felt realistic compared to my actual experience. Unnaturalness: The haptic feedback felt unnatural. Liking: I prefer this haptic feedback. Immersion: I was fully immersed in the virtual environment. Participants provided evaluations on a 0-100 scale (0: strongly disagree, 100: strongly agree) after each session. Additionally, they were given the opportunity to provide subjective comments on their experiences for each session.

5.1.4 Task and Procedure

Before conducting the experiment, participants read an experimental manual, and the experimenter explained the nature of the experiment verbally. Prior to participating in the experiment, the participants conducted a calibration to determine the position at which the pedestal device could make the best contact. This was necessary due to variations in hand size among different users. The stimulation point of the pedestal actuator was situated on the palm, and once a stimulation was received at a specific location, the stimulation would remain fixed at that same position. The room temperature was maintained at 25 . To control noise or other information produced by the haptic device, the participants wore noise-cancelling headphones emitting white noise.

The two virtual environments were provided in two separate sessions. The experiment consists of two main sessions: training sessions and the main session. First, in the training session, participants become familiar with the process of picking up objects in the virtual environment using the Granite Stones session. Participants went the virtual experience with a wearable haptic device on their right hand. During this experimental session, thermal feedback was not provided to the user. In the first session, users familiarized themselves with the haptic device by touching and grasping objects in both virtual environments using hand tracking. Thermal feedback was disabled during the practice session, and only encounter-type force feedback was provided. In the

second session, users experienced the four different environments in the virtual setting. To eliminate the influence of noise, participants wore noise-canceling headsets. They were asked to freely touch or interact with objects in each environment for a minimum of 3 minutes. In the second session, to avoid the influence of the order of thermal rendering presentations, two virtual environments were provided randomly for each participant. After every trial, participants evaluated their subjective experience after sufficiently using the haptic device. Participants were given a rest period of at least 3 minutes between each session. The experiment was conducted over an average duration of 45 minutes.

5.2 Result

For the statistical analysis, we utilized a one-way repeated measures ANOVA for each of the variables: Realism, Unnaturalness, Liking, and Immersion. Detailed results are provided below.

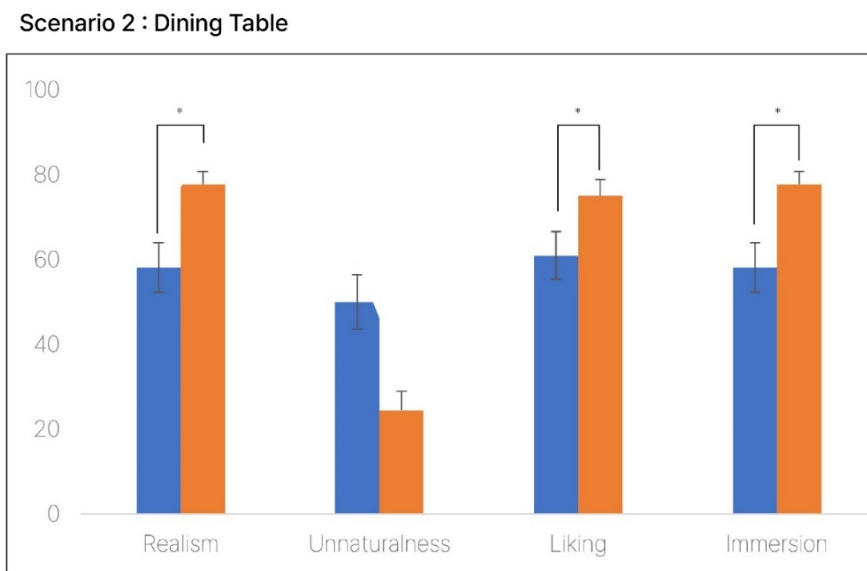
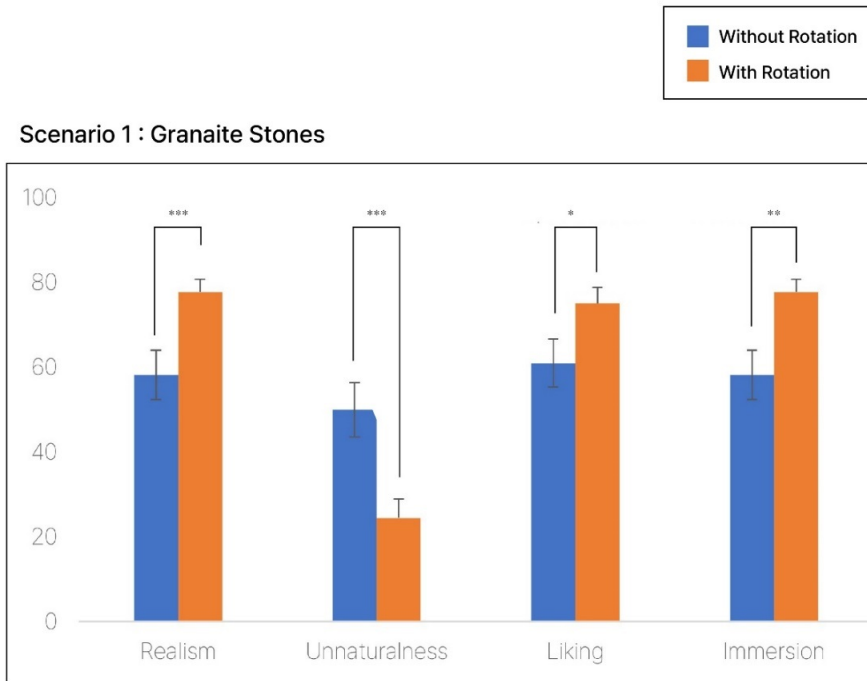


Figure 5.11: User experiment result(*mean $p < 0.05$, **mean $p < 0.01$)

Question	t	df	p
Realism*	5.08	11	<0.001
Unnaturalness*	5.27	11	<0.001
Liking*	2.86	11	0.016
Immersion*	4.01	11	0.002

Table 5.1: Results of 'Granite Stones' (statistically significant terms are marked by *)

Question	t	df	p
Realism*	2.77	11	0.018
Unnaturalness	1.78	11	0.103
Liking*	2.99	11	0.012
Immersion*	3.24	11	0.008

Table 5.2: Results of 'Dinning Table' (statistically significant terms are marked by *)

5.3 Discussion

This study was conducted to evaluate the user experience with and without the Rotation System to achieve rapid satisfaction for initial speed. In Scenario 1, there were significant differences observed in Realism, Unnaturalness, Liking, and Immersion. In Scenario 2, With Rotation received higher ratings than Without Rotation for all evaluation criteria, and significant differences were noted in Realism, Immersion, and Liking. The results confirmed that reducing the time it takes to reach the initial temperature within a shorter period leads to a more positively perceived cognitive experience.

VI. Example Applications

There are countless applications in which our multi-modal haptic device can be utilized. We have created three demo experiences that can be categorized into three popular categories of VR applications : social app, education, and simulator.

6.1 Social Apps

One of the significant challenges in applications that involve interacting with others is the difficulty in providing feedback beyond the auditory sense in social interactions. To demonstrate the usability of our device as a social app, we developed a social game within a virtual environment where users can engage in playful snow fighting. Our device enables feedback during interactions such as throwing snowball or handshakes with the other participant.



Figure 6.1: We designed a game that allows users to engage in snow fighting, and experience social skinship

6.2 Education

To enhance user engagement with realistic scenarios in a virtual environment, we created a fire simulation that users can experience alongside our custom-made haptic thermal feedback device. Traditional evacuation training often lacks immersive engagement due to the absence of direct experience in risky situations. For example, if a doorknob feels hot, it signifies fire on the other side and prompts the need to avoid opening it, using an alternative exit. However, without a haptic device, reproducing such situations in a virtual environment is challenging. We offer this practical feedback in our designed application. Using customizable templates that simulate varying levels of heat based on fire size, users can experience different levels of thermal sensation and conduct more realistic evacuation training.



Figure 6.2: In this demonstration, we simulated a scenario where a fire occurs indoors

6.3 Simulator

While most people cannot physically travel to planets beyond Earth, we can replicate tactile sensations using collected data through simulations. By utilizing physics engines, haptic modeling, rendering, and hardware, we can provide users with sensory experiences involving sight, heat, and tactile feedback, allowing them to reproduce and train for phenomena in space exploration, like differing gravities or surface textures of other planets. Our application allows users to experience the sensation of objects with varying weights due to different planetary gravities, or the feeling of touching the lunar soil or Martian surface.



Figure 6.3: Our space simulation which enables users to interact with objects synchronized with the gravitational forces and atmospheric temperatures of external planets

VII. Conclusion and Future Work

7.1 Conclusion

To our knowledge, there has been no attempt to use multiple pedestal devices to rapidly adjust the initial temperature as described. Conventional devices for perceiving object temperature in virtual environments have significant delays in responding to sudden changes in heat flux, which limits the overall user experience improvement. In this study, we propose a wearable thermal rendering system that alleviates these issues by preheating multiple Peltier elements and providing dynamic thermal feedback. The system determines the heat flux for the contacted object in real-time and controls the preheated haptic interface to provide thermal sensations. In a user experiment evaluating the subjective quality of the developed system compared to conventional thermal rendering methods, our system demonstrated more positive user experiences in scenarios involving contact with objects and receiving thermal feedback.

7.2 Limitations

- The proposed hardware adopts a synchronization method that synchronizes the initial temperature with the heat amount at the moment of contact with the hand. This method, when applied to materials with high thermal conductivity like copper or aluminum which need to be maintained at a lower temperature, encounters issues. The proposed device has a relatively lower thermal conductivity and is not an infinite medium, causing it to heat up more than intended, leading to discrepancies with the desired rendering curve.
- The stimulation is limited to the palm, posing restrictions on the actions possible when gripping, a limitation in itself.

- In situations where the temperature must change continuously on the thermal display, the rotation mechanism cannot be used. This aspect makes it equivalent in effect to using a single thermal display when expressing changes in ambient temperature, radiant heat energy, or when an object has to undergo rapid temperature changes.
- Using four Peltier devices has made the hardware physically heavier, negatively affecting usability. The heaviness of the objects may be burdensome for general users to use continuously. Therefore, a lightweight design is an essential factor in enhancing the user experience.

7.3 Future Work

- **System implementation for more accurate rendering**

When the hand and the Peltier device collide in an encounter-type scenario, the bigger the initial temperature difference between the skin and the Peltier device, the more significant the temperature difference in the Peltier device. Below is a temperature result graph when the amount of surface area was adjusted and made to contact the palm. We can observe that the graph, which previously did not converge within 5 seconds, now aligns. Thus, if there's a display that can adjust the contact surface area based on the material one aims to represent, it would be possible to render the heat more accurately.

- **Improvement to increase the rate of temperature decrease and increase**

If the speed of temperature decrease or increase can be enhanced, the graph can be estimated more accurately. For example, a multi-layer designed Peltier device can maintain the opposite side of the Peltier display at a colder temperature than the ambient temperature[?]. Consequently, in this case, compared to a single Peltier device, the cooling rate is faster and the heating rate is slower.

- **Proposal of a complex thermal source representation method viable in real-**

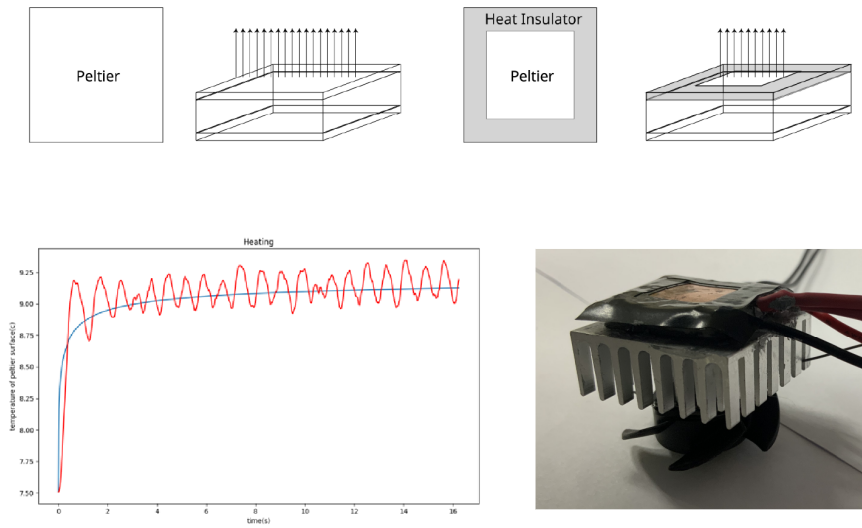


Figure 7.1: Thermal Rendering Results at 10 Degrees of Aluminum with Reduced Contact Area

time environments

Currently, objects with complex structures are transformed into similar objects, and users individually specify and check parameters to determine the representation. If a model is developed that can predict the temperature outcome in real-time when holding a single object, it would aid in providing a more realistic experience for users in virtual environments.

요약문

가상 환경에서 피부 온도와 다른 물체와 손이 접촉하는 과정에서의 열 교환 경험을 사용자에게 사실적으로 제공하기 위해서는 2가지의 조건이 만족되어야 한다. 첫 번째 조건은 조우형 햅틱 피드백을 제공해야한다는 것, 두 번째 조건은 접촉 시간에 따라 피부에 열 유속이 동일하게 제공 되어야 한다는 것이다. 이 조건들을 만족하기 위해서는 열 디스플레이가 표현하려는 재질에 따라 다른 초기 온도로 변화 된 상태에서 피부와 접촉해야하는데 이 조건을 만족하기 위해 열 디스플레이가 온도를 변화하는 과정에서 지연 시간이 발생한다. 본 연구에서는 다수의 펠티어 소자를 예열해놓고 열감 변화를 제공하는 착용형 장치를 제안하였고 기존의 제 착용형 장치들 보다 초기 온도에 대한 도달 지연 시간을 낮출 수 있다는 것을 밝혔다. 기존의 열감 렌더링 방법과 비교하여 본 연구에서 제시한 시스템의 주관적 품질을 평가하기 위해 사용자 실험을 진행하였고 물체와 접촉하여 온도를 제공 받는 열 전도 상황에 대하여 우리의 시스템이 비교 시스템보다 더 긍정적인 사용자 경험을 제공함을 확인하였다.

References

- [1] Nimesha Ranasinghe, Pravar Jain, Shienny Karwita, David Tolley, and Ellen Yi-Luen Do. Ambiotherm: enhancing sense of presence in virtual reality by simulating real-world environmental conditions. In *Proceedings of the 2017 CHI conference on human factors in computing systems*, pages 1731–1742, 2017.
- [2] Emily Shaw, Tessa Roper, Tommy Nilsson, Glyn Lawson, Sue VG Cobb, and Daniel Miller. The heat is on: Exploring user behaviour in a multisensory virtual environment for fire evacuation. In *Proceedings of the 2019 CHI Conference on Human Factors in Computing Systems*, pages 1–13, 2019.
- [3] Cathy Fang, Yang Zhang, Matthew Dworman, and Chris Harrison. Wireality: Enabling complex tangible geometries in virtual reality with worn multi-string haptics. In *Proceedings of the 2020 CHI Conference on Human Factors in Computing Systems*, pages 1–10, 2020.
- [4] Jongyoon Lim and Yongsoon Choi. Force-feedback haptic device for representation of tugs in virtual reality. *Electronics*, 11(11):1730, 2022.
- [5] Jaeyeon Lee, Mike Sinclair, Mar Gonzalez-Franco, Eyal Ofek, and Christian Holz. Torc: A virtual reality controller for in-hand high-dexterity finger interaction. In *Proceedings of the 2019 CHI conference on human factors in computing systems*, pages 1–13, 2019.
- [6] Inrak Choi, Eyal Ofek, Hrvoje Benko, Mike Sinclair, and Christian Holz. Claw: A multifunctional handheld haptic controller for grasping, touching, and triggering in virtual reality. In *Proceedings of the 2018 CHI conference on human factors in computing systems*, pages 1–13, 2018.

- [7] Hrvoje Benko, Christian Holz, Mike Sinclair, and Eyal Ofek. Normaltouch and texturetouch: High-fidelity 3d haptic shape rendering on handheld virtual reality controllers. In *Proceedings of the 29th annual symposium on user interface software and technology*, pages 717–728, 2016.
- [8] Eric Whitmire, Hrvoje Benko, Christian Holz, Eyal Ofek, and Mike Sinclair. Haptic revolver: Touch, shear, texture, and shape rendering on a reconfigurable virtual reality controller. In *Proceedings of the 2018 CHI conference on human factors in computing systems*, pages 1–12, 2018.
- [9] Jas Brooks, Steven Nagels, and Pedro Lopes. Trigeminal-based temperature illusions. In *Proceedings of the 2020 CHI conference on human factors in computing systems*, pages 1–12, 2020.
- [10] Bowen Zhang and Misha Sra. Pneumod: A modular haptic device with localized pressure and thermal feedback. In *Proceedings of the 27th ACM Symposium on Virtual Reality Software and Technology*, pages 1–7, 2021.
- [11] Sosuke Ichihashi, Arata Horie, Masaharu Hirose, Zendai Kashino, Shigeo Yoshida, Sohei Wakisaka, and Masahiko Inami. Thermoblinds: Non-contact, highly responsive thermal feedback for thermal interaction. In *ACM SIGGRAPH 2022 Emerging Technologies*, pages 1–2. 2022.
- [12] Yuhu Liu, Satoshi Nishikawa, Young Ah Seong, Ryuma Niiyama, and Yasuo Kuniyoshi. Thermocaress: A wearable haptic device with illusory moving thermal stimulation. In *Proceedings of the 2021 CHI Conference on Human Factors in Computing Systems*, pages 1–12, 2021.
- [13] Roshan Lalintha Peiris, Wei Peng, Zikun Chen, Liwei Chan, and Kouta Minamizawa. Thermovr: Exploring integrated thermal haptic feedback with head mounted displays. In *Proceedings of the 2017 CHI Conference on Human Factors in Computing Systems*, pages 5452–5456, 2017.

- [14] Barbara Deml, Andreas Mihalyi, and Gunter Hannig. Development and experimental evaluation of a thermal display. In *Proc. EuroHaptics Conf*, pages 257–262. Citeseer, 2006.
- [15] Eliana B Souto, Joana F Fangueiro, Ana R Fernandes, Amanda Cano, Elena Sanchez-Lopez, Maria L Garcia, Patrícia Severino, Maria O Paganelli, Marco V Chaud, and Amélia M Silva. Physicochemical and biopharmaceutical aspects influencing skin permeation and role of sln and nlc for skin drug delivery. *Heliyon*, 2022.
- [16] Shigeki Nomoto, Masaaki Shibata, Masami Iriki, and Walter Riedel. Role of afferent pathways of heat and cold in body temperature regulation. *International journal of biometeorology*, 49:67–85, 2004.
- [17] Lynette A Jones and Michal Berris. The psychophysics of temperature perception and thermal-interface design. In *Proceedings 10th symposium on haptic interfaces for virtual environment and teleoperator systems. HAPTICS 2002*, pages 137–142. IEEE, 2002.
- [18] Ian Darian-Smith and Kenneth O Johnson. Thermal sensibility and thermoreceptors. *Journal of Investigative Dermatology*, 69(1):146–153, 1977.
- [19] David C Spray. Cutaneous temperature receptors. *Annual review of physiology*, 48(1):625–638, 1986.
- [20] DR Kenshalo. Correlations of temperature sensitivity in man and monkey, a first approximation. In *Sensory functions of the skin in primates*, pages 305–330. Elsevier, 1976.
- [21] JOSEPH C. STEVENS KENNETH K. CHOO. Temperature sensitivity of the body surface over the life span. *Somatosensory & motor research*, 15(1):13–28, 1998.

- [22] Kenneth O Johnson, Ian Darian-Smith, and Carole LaMotte. Peripheral neural determinants of temperature discrimination in man: a correlative study of responses to cooling skin. *Journal of Neurophysiology*, 36(2):347–370, 1973.
- [23] KO Johnson, I Darian-Smith, C LaMotte, B Johnson, and S Oldfield. Coding of incremental changes in skin temperature by a population of warm fibers in the monkey: correlation with intensity discrimination in man. *Journal of Neurophysiology*, 42(5):1332–1353, 1979.
- [24] Lynette A Jones and Michal Berris. Material discrimination and thermal perception. In *11th Symposium on Haptic Interfaces for Virtual Environment and Teleoperator Systems, 2003. HAPTICS 2003. Proceedings.*, pages 171–178. IEEE, 2003.
- [25] RONALD VERRILLO, STANLEY BOLANOWSKI, CHRISTINE FRANCIS, and FRANCIS McGLONE. Effects of hydration on tactile sensation. *Somatosensory & motor research*, 15(2):93–108, 1998.
- [26] Hsin-Ni Ho. Material recognition based on thermal cues: Mechanisms and applications. *Temperature*, 5(1):36–55, 2018.
- [27] Hsin-Ni Ho and Lynette A Jones. Modeling the thermal responses of the skin surface during hand-object interactions. 2008.
- [28] Gi-Hun Yang, Dong-Soo Kwon, and Lynette A Jones. Spatial acuity and summation on the hand: The role of thermal cues in material discrimination. *Perception & Psychophysics*, 71(1):156–163, 2009.
- [29] Gi-Hun Yang, Lynette A Jones, and Dong-Soo Kwon. Use of simulated thermal cues for material discrimination and identification with a multi-fingered display. *Presence: Teleoperators and Virtual Environments*, 17(1):29–42, 2008.
- [30] Mohamed Benali-Khoudjal, Moustapha Hafez, J-M Alexandre, Jamil Benachour, and Abderrahmane Kheddar. Thermal feedback model for virtual reality.

- In *MHS2003. Proceedings of 2003 International Symposium on Micromechanics and Human Science (IEEE Cat. No. 03TH8717)*, pages 153–158. IEEE, 2003.
- [31] Massimo Bergamasco, Alessio A Alessi, and Maurizio Calcarà. Thermal feedback in virtual environments. *Presence: Teleoperators & Virtual Environments*, 6(6):617–629, 1997.
- [32] Alexander Kron and Günther Schmidt. Multi-fingered tactile feedback from virtual and remote environments. In *11th Symposium on Haptic Interfaces for Virtual Environment and Teleoperator Systems, 2003. HAPTICS 2003. Proceedings.*, pages 16–23. IEEE, 2003.
- [33] Healthcare Additive Manufacturing Market Size. Share & trends analysis report by technology (laser sintering, stereolithography), by application (medical implants, prosthetics), by material, and segment forecasts, 2022–2030. *Grand View Research: San Francisco, CA, USA, 2022.*
- [34] Shaoyu Cai, Pingchuan Ke, Takuji Narumi, and Kening Zhu. Thermairglove: A pneumatic glove for thermal perception and material identification in virtual reality. In *2020 IEEE conference on virtual reality and 3D user interfaces (VR)*, pages 248–257. IEEE, 2020.
- [35] Seung-Won Kim, Sung Hee Kim, Choong Sun Kim, Kyoungsoo Yi, Jun-Sik Kim, Byung Jin Cho, and Youngsu Cha. Thermal display glove for interacting with virtual reality. *Scientific reports*, 10(1):11403, 2020.
- [36] Jinhyeok Oh, Suin Kim, Sangyeop Lee, Seongmin Jeong, Seung Hwan Ko, and Joonbum Bae. A liquid metal based multimodal sensor and haptic feedback device for thermal and tactile sensation generation in virtual reality. *Advanced Functional Materials*, 31(39):2007772, 2021.

- [37] Michael Smith, Vito Cacucciolo, and Herbert Shea. Fiber pumps for wearable fluidic systems. *Science*, 379(6639):1327–1332, 2023.
- [38] Teng Han, Fraser Anderson, Pourang Irani, and Tovi Grossman. Hydroring: Supporting mixed reality haptics using liquid flow. In *Proceedings of the 31st Annual ACM Symposium on User Interface Software and Technology*, pages 913–925, 2018.
- [39] Abdallah El Ali, Xingyu Yang, Swamy Ananthanarayan, Thomas Röggl, Jack Jansen, Jess Hartcher-O’Brien, Kaspar Jansen, and Pablo Cesar. Thermalwear: Exploring wearable on-chest thermal displays to augment voice messages with affect. In *Proceedings of the 2020 CHI Conference on Human Factors in Computing Systems*, pages 1–14, 2020.
- [40] Kening Zhu, Simon Perrault, Taizhou Chen, Shaoyu Cai, and Roshan Lalitha Peiris. A sense of ice and fire: Exploring thermal feedback with multiple thermoelectric-cooling elements on a smart ring. *International Journal of Human-Computer Studies*, 130:234–247, 2019.
- [41] Roshan Lalitha Peiris, Yuan-Ling Feng, Liwei Chan, and Kouta Minamizawa. Thermalbracelet: Exploring thermal haptic feedback around the wrist. In *Proceedings of the 2019 CHI Conference on Human Factors in Computing Systems*, pages 1–11, 2019.
- [42] Arshad Nasser, Kening Zhu, and Sarah Wiseman. Thermo-haptic earable display for the hearing and visually impaired. In *Proceedings of the 21st International ACM SIGACCESS Conference on Computers and Accessibility*, pages 630–632, 2019.
- [43] Jiayi Xu, Yoshihiro Kuroda, Shunsuke Yoshimoto, and Osamu Oshiro. Non-contact cold thermal display by controlling low-temperature air flow generated

- with vortex tube. In *2019 IEEE World Haptics Conference (WHC)*, pages 133–138. IEEE, 2019.
- [44] Yatharth Singhal, Haokun Wang, Hyunjae Gil, and Jin Ryong Kim. Mid-air thermo-tactile feedback using ultrasound haptic display. In *Proceedings of the 27th ACM Symposium on Virtual Reality Software and Technology*, pages 1–11, 2021.
- [45] Sebastian Günther, Florian Müller, Dominik Schön, Omar Elmoghazy, Max Mühlhäuser, and Martin Schmitz. Terminator: Understanding the interdependency of visual and on-body thermal feedback in virtual reality. In *Proceedings of the 2020 CHI Conference on Human Factors in Computing Systems*, pages 1–14, 2020.
- [46] Lynette A Jones and Hsin-Ni Ho. Warm or cool, large or small? the challenge of thermal displays. *IEEE Transactions on Haptics*, 1(1):53–70, 2008.
- [47] Shuichi Ino, Shunji Shimizu, Tetsuro Odagawa, Mitsuru Sato, M Takahashi, T Izumi, and T Ifukube. A tactile display for presenting quality of materials by changing the temperature of skin surface. In *Proceedings of 1993 2nd IEEE International Workshop on Robot and Human Communication*, pages 220–224. IEEE, 1993.
- [48] Akio Yamamoto, Benjamin Cros, Hironori Hashimoto, and Toshiro Higuchi. Control of thermal tactile display based on prediction of contact temperature. In *IEEE International Conference on Robotics and Automation, 2004. Proceedings. ICRA'04. 2004*, volume 2, pages 1536–1541. IEEE, 2004.
- [49] H Ho and LA Jones. Material identification using real and simulated thermal cues. In *The 26th annual international conference of the IEEE engineering in medicine and biology society*, volume 1, pages 2462–2465. IEEE, 2004.

- [50] Darwin G Caldwell and Clarence Gosney. Enhanced tactile feedback (teletaction) using a multi-functional sensory system. In *[1993] Proceedings IEEE International Conference on Robotics and Automation*, pages 955–960. IEEE, 1993.
- [51] Johann Citérin, Aurélien Pocheville, and Abderrahmane Kheddar. A touch rendering device in a virtual environment with kinesthetic and thermal feedback. In *Proceedings 2006 IEEE International Conference on Robotics and Automation, 2006. ICRA 2006.*, pages 3923–3928. IEEE, 2006.
- [52] George L Wilcox and Glenn J Giesler Jr. An instrument using a multiple layer peltier device to change skin temperature rapidly. *Brain research bulletin*, 12(1):143–146, 1984.

Acknowledgements

2년간 지도 편달을 주신 최승문 교수님께 가장 먼저 감사의 인사를 올립니다. 교수님과 연구실 동료들을 보며 많은 것을 보고 느끼며 연구자로서의 태도와 관점이 무엇인지에 대해 조금이나마 엿보며 2년을 보낼 수 있었습니다. 교수님의 학자로서의 열정과 험퍽에 대한 다양한 연구를 수행하는 인터랙션 연구실 인원들과 함께 할 수 있던 것이 큰 행운이라 생각합니다. 지도해주신 최승문 교수님께서 석사 기간 동안 하나의 주제에 대해 깊이 있게 연구를 수행했으면 한다고 지속적으로 자극을 주시고 연구실 동료들로부터 자극을 받았기에 부족한 제가 그 말의 무게와 가치를 조금이나마 느낄 수 있었습니다.

지도 교수님과 함께 연구를 수행하는데 있어 여러 방향에서 자극과 조언을 아끼지 않고 주셨던 오승재 교수님, 또한 귀한 시간을 내주시며 저의 석사 졸업 논문을 심사해주시며 피드백을 주셨던 황인석, 김옥성 교수님들 감사드립니다.

연구실에 처음 왔을 때의 랩장으로서 적응하는 것을 챙겨주던 겨레, 여러가지 연구 조언을 아낌없이 주던 채용, 부족한 점들에 대해 적극적인 피드백을 주던 지원, 이런 저런 메이킹 정보들을 주던 정은, 가끔씩 뜬금 없는 걱정과 응원의 말을 주는 것이 고마웠던 다진, 적극적으로 리드하는 모습을 보여주며 틈틈이 챙겨주던 동근, 진심 어린 응원을 해주던 정우, 옆 자리에 앉아서 말동무 해주던 재준, 함께 CT 과제를 비롯하여 2년여간을 동고동락한 준우, 수업을 같이 들으며 이런 저런 이야기를 나누던 재혁과 희연, 디펜스가 끝나고 나서야 이야기를 나눠볼 수 있던 희지, 그리고 행정을 담당해 주신 예지 선생님을 비롯해 연구실 동료들 모두 감사합니다. 마지막으로 저를 응원하고 지지 해준 가족들에게 감사의 마음을 전합니다.

Curriculum Vitae

Name : Hoseok Jung

Education

2015. 03. – 2021. 08. Department of Painting, Industrial Design, Computer Engineering, Electronic and Electrical Engineering, Hongik University (B.F.A , B.S.)

2021. 09. – 2023. 08. Department of Computer Science and Engineering, Pohang University of Science and Technology (M.S.)

